

Bethe-Salpeter Approach for Unitarized Chiral Perturbation Theory.

J. Nieves and E. Ruiz Arriola

*Departamento de Física Moderna
Universidad de Granada
E-18071 Granada, Spain
(March 9, 2022)*

The Bethe-Salpeter equation restores exact elastic unitarity in the s -channel by summing up an infinite set of chiral loops. We use this equation to show how a chiral expansion can be undertaken in the two particle irreducible amplitude and the propagators accomplishing exact elastic unitarity at any step. Renormalizability of the amplitudes can be achieved by allowing for an infinite set of counter-terms as it is the case in ordinary Chiral Perturbation Theory. Crossing constraints can be imposed on the parameters to a given order. Within this framework, we calculate the leading and next-to-leading contributions to the elastic $\pi\pi$ scattering amplitudes, for all isospin channels, and to the vector and scalar pion form factors in several renormalization schemes. A satisfactory description of amplitudes and form factors is obtained. In this latter case, Watson's theorem is automatically satisfied. From such studies we obtain a quite accurate determination of some of the ChPT $SU(2)$ -low energy parameters ($\bar{l}_1 - \bar{l}_2 = -6.1_{-0.3}^{+0.1}$ and $\bar{l}_6 = 19.14 \pm 0.19$). We also compare the two loop piece of our amplitudes to recent two-loop calculations.

PACS: 11.10.St; 11.30.Rd; 11.80.Et; 13.75.Lb; 14.40.Cs; 14.40.Aq

Keywords: Bethe-Salpeter Equation, Chiral Perturbation Theory, Unitarity, $\pi\pi$ -Scattering, Resonances.

I. INTRODUCTION

The dynamical origin of resonances in $\pi\pi$ scattering has been a recurrent subject in low energy particle physics [1]. Analyticity, unitarity, crossing and chiral symmetry have provided main insights into this subject. It is well known that so far no solution is available exactly fulfilling all these requirements. In practical calculations some of the properties mentioned above have to be given up. Standard Chiral Perturbation Theory (ChPT) furnishes exact crossing and restores unitarity order by order in the chiral expansion. In typical calculations the unitarity limit is reached at about a center of mass (CM) energy $\sqrt{s} \sim 4\sqrt{\pi}f \sim 670 \text{ MeV}^1$ still a low scale compared to the known resonances. Simply because of this reason standard ChPT is unable to describe the physically observed resonances, namely the ρ and the σ . But even if the unitarity limit was much larger, and thus resonances would appear at significantly smaller scales than it, standard ChPT would be unable to generate them since its applicability requires the existence of a gap between the pion states and the hadronic states next in energy, which for $\pi\pi$ scattering are precisely the resonances. Resonances clearly indicate the presence of non perturbative physics, and thus a pole on the second Riemann sheet (signal of the resonance) cannot be obtained in perturbation theory to finite order. Hence, the energy regime for which ChPT holds has to satisfy $s \ll m_R^2$ regardless of the unitarity limit. It so happens that both the resonances and the unitarity limit lead to similar scales, but there is so far no compelling reason to ascribe this coincidence to some underlying dynamical feature or symmetry².

The desire to describe resonances using standard ChPT as a guide has led some authors to propose several approaches which favor some of the properties, that the exact scattering amplitude should satisfy, respect to others. Thus, Pade Re-summation (PR) [2], Large N_f -Expansion (LNE) [3], Inverse Amplitude Method (IAM) [4], Current Algebra Unitarization (CAU) [5], Dispersion Relations (DP) [6], Roy Equations [7], Coupled Channel Lippmann-Schwinger Approach (CCLS) [8] and hybrid approaches [9] have been suggested. Besides their advantages and success to describe the data in the low-lying resonance region, any of them has specific drawbacks. In all above approaches except by LNE and CCLS it is not clear which is the ChPT series of diagrams which has been summed up. This is not the case for the CCLS approach, but there a three momentum cut-off is introduced, hence breaking translational Lorentz invariance and therefore the scattering amplitude can be only evaluated in the the CM frame. On the other hand, though the LNE and CAU approaches preserve crossing symmetry, both of them violate unitarity. Likewise, those approaches which preserve exact unitarity violate crossing symmetry.

A clear advantage of maintaining elastic unitarity lies in the unambiguous identification of the phase shifts. This is particularly useful to describe resonances since the modulus of

¹Through this paper m is the pion mass, for which we take 139.57 MeV, and f the pion decay constant, for which we take 93.2 MeV.

²To see this, consider for instance the large N_c limit where $f \sim \sqrt{N_c}$ but $m_R \sim N_c^0$ and $\Gamma_R \sim 1/N_c$, so in this limit $f \gg m_R$, which suggests a possible scenario where resonances can appear well below the unitarity limit.

the partial wave amplitude reaches at the resonant energy the maximum value allowed by unitarity. On the other hand, a traditional objection to any unitarization scheme is provided by the non-uniqueness of the procedure; this ambiguity is related to our lack of knowledge of an appropriate expansion parameter for resonant energy physics. This drawback does not invalidate the systematics and predictive power of unitarization methods, although it is true that improvement has a different meaning for different schemes. In addition, unitarization by itself is not sufficient to predict a resonance, some methods work while others do not. Against unitarization it is also argued that since crossing symmetry is violated, the connection to a Lagrangian framework is lost, and hence there is no predictive power for other processes in terms of a few phenomenological constants.

The Bethe-Salpeter equation (BSE) provides a natural framework beyond perturbation theory to treat the relativistic two body problem from a Quantum Field Theory (QFT) point of view [10]. This approach allows to treat both the study of the scattering and of the bound state properties of the system. In practical applications, however, approximations have to be introduced which, generally speaking, violate some known properties of the underlying QFT. This failure only reflects our in-capability of guessing the exact solution. The problem with the truncations is that almost always the micro-causality requirement is lost, and hence the local character of the theory. As a consequence, properties directly related to locality such as CPT, crossing and related ones are not exactly satisfied. This has led some authors to use the less stringent framework of relativistic quantum mechanics as a basis to formulate the few body problem [11]. It would be, of course, of indubitable interest the formulation of a chiral expansion within such a framework.

Despite of these problems, even at the lowest order approximation, or ladder approximation, the BSE sums an infinite set of diagrams, allowing for a manifest implementation of elastic unitarity. This is certainly very relevant in the scattering region and more specifically if one aims to describe resonances, as we have discussed above. At higher orders, to implement unitarity one needs to include inelastic processes due to particle production ($\pi\pi \rightarrow K\bar{K}$, $\pi\pi \rightarrow \pi\pi\pi\pi, \dots$).

In general, the renormalization of the BSE is a difficult problem for QFT's in the continuum. The complications arise because typical local features, i.e. properties depending on micro-causality, like crossing are broken by the approximate nature of the solution. This means that there is no a renormalized Lagrangian which *exactly* reproduces the amplitude, but only up to the approximate level of the solution. This is the price payed for manifest unitarity. Fortunately, from the point of view of the Effective Field Theory (EFT) idea, this problem can be tackled in a manageable and analytical way. Since this is a low energy expansion in terms of the appropriate relevant degrees of freedom, interactions are suppressed in powers of momentum and thus the BSE equation can be solved and renormalized explicitly by expanding the iterated two particle irreducible amplitude in a power series of momentum. This requires the introduction of a finite number of counter-terms for a given order in the expansion. The higher the order in this expansion, the larger the number of parameters, and thus the predictive power of the expansion diminishes. Thus an acceptable compromise between predictive power and degree of accuracy has to be reached. Within the

BSE such a program, although possible, has the unpleasant feature of arbitrariness in the renormalization scheme, although this is also the case in standard ChPT³.

In this paper we study the scattering of pseudoscalar mesons by means of the BSE in the context of ChPT. Most useful information can be extracted from chiral symmetry, which dictates the energy dependence of the scattering amplitude as a power series expansion of $1/f^2$. The unknown coefficients of the expansion increase with the order. By using the BSE we can also predict the energy dependence of the scattering amplitude in terms of unknown coefficients and in agreement with the unitarity requirement. This can be done in a way to comply with the known behavior in ChPT.

One important outcome of our calculation is the justification of several methods based on algebraic manipulations of the on-shell scattering amplitude, and which make no reference to the set of diagrams which are summed up. Moreover, some off-shell quantities are obtained. Although it is true that physical quantities only make sense when going to the mass shell there is no doubt that off-shell quantities do enter into few body calculations.

Among others, the main results of the present investigation are the following ones:

- A quantitative accurate description of both pion form factors and $\pi\pi$ elastic scattering amplitudes is achieved in an energy region wider than the one in which ChPT works. We implement exact elastic unitarity whereas crossing symmetry is perturbatively restored. For the form factors, the approach presented here automatically satisfies Watson's theorem and it goes beyond the leading order Omnès representation which is traditionally used.
- A meticulous error treatment is undertaken. Our investigations on the pion electric form factor together with our statistical and systematic error analysis provide a very accurate determination of some of the ChPT $SU(2)$ -low energy parameters,

$$\bar{l}_1 - \bar{l}_2 = -6.1_{-0.3}^{+0.1}, \quad \bar{l}_6 = 19.14 \pm 0.19$$

- The current approach reproduces ChPT to one loop. However and mainly due to the precise determination of the difference $\bar{l}_1 - \bar{l}_2$ quoted above, our one loop results have much smaller errors than most of the previously published ones. As a consequence, we generate some of the two-loop corrections more precisely than recent two loop calculations do.
- The present framework allows for an improvement of any computed order of ChPT.

The paper is organized as follows. In Sect. II we discuss the BSE for the case of scattering of pseudoscalar mesons together with our particular conventions and definitions. In Sect. III we review and improve the lowest order solution for the off-shell amplitudes, found in a previous work [12]. We also show that, already at this level, a satisfactory description

³There, higher order terms than the computed ones are exactly set to zero. This choice is as arbitrary as any other one where these higher order terms are set different from zero. The advantages of taking them different from zero as dictated by unitarity will become clear along the paper.

of data can be achieved when a reasonable set of ChPT low energy parameters is used. This is done in Subsect. III F. Technical details are postponed to Appendix A. The computation of the next-to-leading order corrections, within this off-shell scheme, turns out to be rather cumbersome. The difficulties can be circumvented by introducing what we call the “on-shell” scheme, as we do in Sect. IV. After having discussed some renormalization issues, the decoupling of the off-shell amplitudes is achieved in Subsect. IV C by means of a generalized partial wave expansion. In this context, the renormalization conditions can also be stated in a more transparent way. The findings of Subsect. IV C allow us to write an exact T -matrix if an exact two particle irreducible amplitude was known. In Subsect. IV D, we show that the found solution satisfies off-shell unitarity and in the next two subsections we present several systematic expansions of the two particle irreducible amplitude. In Subsect. IV G, we show how our amplitudes can be fruitfully employed for the calculation of pseudoscalar meson form factors, in harmony with Watson’s theorem. Next-to-leading order numerical results for both $\pi\pi$ scattering and form factors (vector and scalar) are presented in Subsect. IV H. This study allows us to determine, very precisely, the parameters \bar{l}_1, \bar{l}_2 (specially their difference) and \bar{l}_6 from experimental data. Besides, we also compare with recent two-loop calculations. In Subsect. IV I we compare some results obtained at leading and next-to-leading accuracy, within the BSE on-shell scheme. Such a study tests the convergence of the approach presented in this work. In Sect. V we try to understand qualitatively the origin of some renormalization constants which naturally appear within the BSE approach and in particular a remarkable formula for the width of the ρ meson, very similar to the celebrated KSFR, is deduced. In Sect. VI we briefly analyze alternative unitarization methods on the light of the BSE approach. Conclusions are presented in Sect. VII. Finally, in Appendix B the leading and next-to-leading elastic $\pi\pi$ scattering amplitudes in ChPT are compiled and we also give analytical expressions for the u - and t - unitarity chiral corrections projected over both isospin and angular momentum.

II. THE BETHE-SALPETER EQUATION.

Let us consider the scattering of two identical mesons of mass, m . The BSE can, with the kinematics described in Fig. 1, be written as

$$T_P(p, k) = V_P(p, k) + i \int \frac{d^4q}{(2\pi)^4} T_P(q, k) \Delta(q_+) \Delta(q_-) V_P(p, q) \quad (1)$$

where $q_{\pm} = (P/2 \pm q)$ and $T_P(p, k)$ and $V_P(p, k)$ are the total scattering amplitude⁴ and the two particle irreducible amplitude (*potential*) respectively. Besides, Δ is the exact pseudoscalar meson propagator. Note that the previous equation requires knowledge about the

⁴The normalization of the amplitude T is determined by its relation with the differential cross section in the CM system of the two identical mesons and it is given by $d\sigma/d\Omega = |T_P(p, k)|^2/64\pi^2 s$, where $s = P^2$. The phase of the amplitude T is such that the optical theorem reads $\text{Im}T_P(p, p) = -\sigma_{\text{tot}}(s^2 - 4s m^2)^{1/2}$, with σ_{tot} the total cross section. The contribution to the amputated Feynman diagram is $(-iT_P(p, k))$ in the Fig. 1.

off-shell potential and the off-shell amplitude⁵. Clearly, for the exact potential V and propagator Δ the BSE provides an exact solution of the scattering amplitude T [10]. Obviously an exact solution for T is not accessible, since V and Δ are not exactly known. An interesting property, direct consequence of the two particle irreducible character of the potential, is that in the elastic scattering region $s > 4m^2$, V is a real function, and that it also has a discontinuity for $s < 0$, i.e. $t > 4m^2$. We will also see below that, because of the inherent freedom of the renormalization program of an EFT, the definition of the potential is ambiguous, and some reference scale ought to be introduced in general. The exact amplitude, of course, will be scale independent.

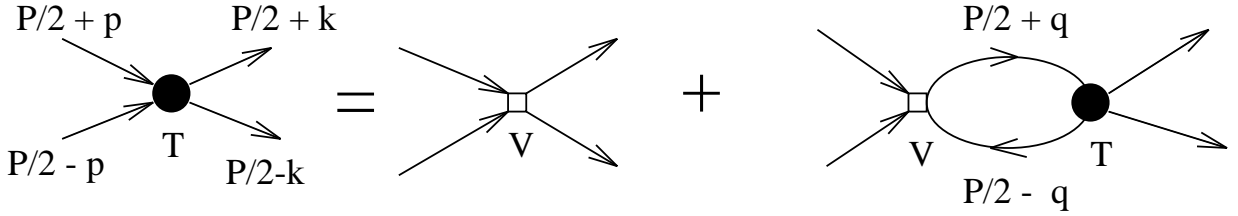


FIG. 1. Diagrammatic representation of the BSE equation. It is also sketched the used kinematics.

Probably, the most appealing feature of the BSE is that it accomplishes the two particle unitarity requirement⁶

$$T_P(p, k) - T_P(k, p)^* = -i(2\pi)^2 \int \frac{d^4q}{(2\pi)^4} T_P(q, k) \delta^+(q_+^2 - m^2) \delta^+(q_-^2 - m^2) T_P(q, p)^* \quad (2)$$

as can be deduced from the real character of the potential above threshold $s > 4m^2$, with $\delta^+(p^2 - m^2) = \Theta(p^0)\delta(p^2 - m^2)$. It is important to stress that although the above unitarity condition is considered most frequently for the on-shell amplitude, it is also fulfilled even for off-shell amplitudes. We will see below that these conditions are verified in practice by our amplitudes.

Isospin invariance leads to the following decomposition of the two identical isovector meson scattering amplitude for the process $(P/2 + p, a) + (P/2 - p, b) \rightarrow (P/2 + k, c) + (P/2 - k, d)$,

$$T_P(p, k)_{ab;cd} = A_P(p, k)\delta_{ab}\delta_{cd} + B_P(p, k)\delta_{ac}\delta_{bd} + C_P(p, k)\delta_{ad}\delta_{bc} \quad (3)$$

with a, b, c and d Cartesian isospin indices. With our conventions, the Mandelstam variables are defined as $s = P^2$, $t = (p - k)^2$ and finally $u = (p + k)^2$ and the isospin projection operators, P^I , are given by [13]

⁵We will see later that this off-shellness can be disregarded within the framework of EFT's and using an appropriate regularization scheme.

⁶Cutkosky's rules lead to the substitution $\Delta(p) \rightarrow (-2\pi i)\delta^+(p^2 - m^2)$

$$\begin{aligned}
P_{ab;cd}^0 &= \frac{2}{3}\delta_{ab}\delta_{cd} \\
P_{ab;cd}^1 &= (\delta_{ac}\delta_{bd} - \delta_{ad}\delta_{bc}) \\
P_{ab;cd}^2 &= \left(\delta_{ac}\delta_{bd} + \delta_{ad}\delta_{bc} - \frac{2}{3}\delta_{ab}\delta_{cd} \right)
\end{aligned} \tag{4}$$

The isospin decomposition of the amplitude is then $T_P(p, k)_{ab;cd} = \sum_I P_{ab;cd}^I T_P^I(p, k)$, where

$$\begin{aligned}
T_P^0(p, k) &= \frac{1}{2} (3A_P(p, k) + B_P(p, k) + C_P(p, k)) \\
T_P^1(p, k) &= \frac{1}{2} (B_P(p, k) - C_P(p, k)) \\
T_P^2(p, k) &= \frac{1}{2} (B_P(p, k) + C_P(p, k))
\end{aligned} \tag{5}$$

Based on the identical particle character of the scattered particles we have the following symmetry properties for the isospin amplitudes

$$T_P^I(p, k) = (-)^I T_P^I(p, -k) = (-)^I T_P^I(-p, k) \tag{6}$$

The above relations imply:

$$\begin{aligned}
A_P(p, k) &= A_P(p, -k) = A_P(-p, k) \\
B_P(p, k) &= C_P(p, -k) = C_P(-p, k)
\end{aligned} \tag{7}$$

On the other hand crossing symmetry requires

$$T_P(p, k)_{ab;cd} = T_{(p-k)} \left(\frac{p+k+P}{2}, \frac{p+k-P}{2} \right)_{ac;bd} \tag{8}$$

which implies

$$\begin{aligned}
B_P(p, k) &= A_{(p-k)} \left(\frac{p+k+P}{2}, \frac{p+k-P}{2} \right) \\
C_P(p, k) &= C_{(p-k)} \left(\frac{p+k+P}{2}, \frac{p+k-P}{2} \right)
\end{aligned} \tag{9}$$

Finally crossing, together with rotational invariance also implies:

$$T_P(p, k)_{ab;cd} = T_{-P}(-k, -p)_{cd;ab} = T_{-P}(-k, -p)_{ab;cd} = T_P(k, p)_{ab;cd} \tag{10}$$

which forces to all three functions A_P, B_P and C_P to be symmetric under the exchange of k and p . The relations of Eqs. (7) and (9) can be combined to obtain the standard parameterization on the mass shell:

$$\begin{aligned}
A_P(p, k) &= A(s, t, u) = A(s, u, t) \\
B_P(p, k) &= A(t, s, u) \\
C_P(p, k) &= A(u, t, s)
\end{aligned} \tag{11}$$

On the other hand the relations in Eq. (5) can be inverted, and thus one gets

$$\begin{aligned} A_P(p, k) &= \frac{2}{3} (T_P^0(p, k) - T_P^2(p, k)) \\ B_P(p, k) &= T_P^2(p, k) + T_P^1(p, k) \\ C_P(p, k) &= T_P^2(p, k) - T_P^1(p, k) \end{aligned} \quad (12)$$

Hence, the crossing conditions stated in Eq. (11), impose a set of non trivial relations between the amplitudes $T_P^0(p, k)$, $T_P^1(p, k)$ and $T_P^2(p, k)$.

For comparison with the experimental CM phase shifts, $\delta_{IJ}(s)$, we define the on-shell amplitude for each isospin channel as

$$T^I(s, t) = T_P^I(p, k) ; \quad p^2 = k^2 = m^2 - s/4 ; \quad P \cdot p = P \cdot k = 0 \quad (13)$$

and then the projection over each partial wave J in the CM frame, $T_{IJ}(s)$, is given by

$$T_{IJ}(s) = \frac{1}{2} \int_{-1}^{+1} P_J(\cos \theta) T_P^I(p, k) d(\cos \theta) = \frac{i8\pi s}{\lambda^{\frac{1}{2}}(s, m^2, m^2)} [e^{2i\delta_{IJ}(s)} - 1] \quad (14)$$

where θ is the angle between \vec{p} and \vec{k} in the CM frame, P_J the Legendre polynomials and $\lambda(x, y, z) = x^2 + y^2 + z^2 - 2xy - 2xz - 2yz$. Notice that in our normalization the unitarity limit implies $|T_{IJ}(s)| < 16\pi s / \lambda^{1/2}(s, m^2, m^2)$.

III. OFF-SHELL BSE SCHEME

A. Chiral expansion of the potential and propagator

We propose an expansion along the lines of ChPT both for the exact potential (V) and the exact propagator (Δ),

$$\begin{aligned} \Delta(p) &= \Delta^{(0)}(p) + \Delta^{(2)}(p) + \dots \\ V_P(p, k) &= {}^{(0)}V_P(p, k) + {}^{(2)}V_P(p, k) + \dots \end{aligned} \quad (15)$$

Thus, at lowest order in this expansion, V should be replaced by the $\mathcal{O}(p^2)$ chiral amplitude (${}^{(2)}T$) and Δ by the free meson propagator, $\Delta^{(0)}(r) = (r^2 - m^2 + i\epsilon)^{-1}$. Even at lowest order, by solving Eq. (1) we sum up an infinite set of diagrams. This approach, at lowest order and in the chiral limit reproduces the bubble re-summation undertaken in Ref. [14]. This expansion is related to the approach recently pursued for low energy NN -scattering where higher order t - and u -channel contributions to the potential are suppressed in the heavy nucleon mass limit [15].

To illustrate the procedure, let us consider elastic $\pi\pi$ scattering in the $I = 0, 1, 2$ channels. One word of caution should be said, before proceeding to practical calculations. As one sees the solution of the BSE requires knowledge about off-shell quantities, like the potential, $V_P(p, k)$. This is generally an ambiguous quantity which depends on the particular choice of the pion field. On-shell quantities should however be independent of such a choice. The calculations carried out below correspond to a particular ansatz. A more detailed discussion on other possible choices is postponed to Appendix A 6. The main result is that a judicious choice of the renormalization scheme, leads to on-shell quantities free from this arbitrariness.

1. $I=0$ $\pi\pi$ scattering.

At lowest order, the off-shell potential V in this channel is given by

$$V_P^0(p, k) \approx^{(2)} T_P^0(p, k) = \frac{5m^2 - 3s - 2(p^2 + k^2)}{2f^2} \quad (16)$$

To solve Eq. (1) with the above potential we proceed by iteration. The second Born approximation suggests a solution of the form

$$T_P^0(p, k) = A(s) + B(s)(p^2 + k^2) + C(s)p^2k^2 \quad (17)$$

where $A(s), B(s)$ and $C(s)$ are functions to be determined. Note that, as a simple one loop calculation shows, there appears a new off-shell dependence (p^2k^2) not present in the $\mathcal{O}(p^2)$ potential $^{(2)}T$. That is similar to what happens in standard ChPT [16].

The above ansatz reduces the BSE to a linear algebraic system of four equations with three unknowns (Eq. (A1) in Appendix A). The system turns out to be compatible and the solution of it is given in Eqs. (A5) and (A6) of the Appendix A.

At the lowest order in the chiral expansion examined here, the isoscalar amplitude on the mass shell and in the CM frame ($\vec{P} = 0, p^0 = k^0 = 0, P^0 = \sqrt{s}$) is purely s -wave, and its inverse can be obtained from Eqs. (A5) and (A6). It reads

$$T_{00}^{-1}(s) = -I_0(s) + \frac{2(f^2 + I_2(4m^2))^2}{2I_4(4m^2) + (m^2 - 2s)f^2 + (s - 4m^2)I_2(4m^2)} \quad (18)$$

where $I_0(s)$ is a logarithmically divergent integral, which explicit expression is given in Eq. (A2). Similarly $I_2(4m^2)$ and $I_4(4m^2)$ are divergent quantities, which are defined in terms of the quadratic and quartic divergent integrals $I_2(s)$ and $I_4(s)$ also introduced in Eq. (A2). Thus the above expression for the inverse amplitude requires renormalization, we will back to this point in Subsect. III D.

2. $I=1$ $\pi\pi$ scattering

At lowest order, the off-shell potential V in this channel is approximated by

$$V_P^1(p, k) \approx^{(2)} T_P^1(p, k) = \frac{2p \cdot k}{f^2} \quad (19)$$

As before, to solve Eq. (1) with the above potential we propose a solution of the form

$$T_P^1(p, k) = M(s)p \cdot k + N(s)(p \cdot P)(k \cdot P) \quad (20)$$

where M and N are functions to be determined. Note that, as expected from our previous discussion for the isoscalar case, there appears a new off-shell dependence ($(p \cdot P)(k \cdot P)$) not present in the $\mathcal{O}(p^2)$ potential. Again, this ansatz reduces the BSE to a linear algebraic system of equations which provides the full off-shell scattering amplitude, which is given in Eq. (A7).

At the lowest order presented here, we have only p -wave contribution and the resulting inverse CM amplitude on the mass shell, after angular momentum projection, reads

$$T_{11}^{-1}(s) = -I_0(s) + \frac{2I_2(4m^2) - 6f^2}{s - 4m^2} \quad (21)$$

Similarly to the isoscalar case discussed previously, the above equation presents divergences which need to be consistently renormalized, this issue will be addressed in Subsect. III D.

3. $I=2$ $\pi\pi$ scattering.

At lowest order, the off-shell potential V in this channel is given by

$$V_P^2(p, k) \approx^{(2)} T_P^2(p, k) = \frac{m^2 - (p^2 + k^2)}{f^2} \quad (22)$$

This resembles very much the potential for the isoscalar case, and we search for a solution of the BSE of the form

$$T_P^2(p, k) = A(s) + B(s)(p^2 + k^2) + C(s)p^2k^2 \quad (23)$$

Similarly to the case $I = 0$, the functions $A(s)$, $B(s)$ and $C(s)$ can be readily determined and are given in the Appendix A.

At the lowest order in the chiral expansion examined here, the $I = 2$ amplitude on the mass shell and in the CM frame is purely s -wave, and from Eqs. (A9) and (A10)) we find its inverse reads

$$T_{20}^{-1}(s) = -I_0(s) + \frac{2(f^2 + I_2(4m^2))^2}{2I_4(4m^2) + (s - 2m^2)f^2 + (s - 4m^2)I_2(4m^2)} \quad (24)$$

Once again, the above equation has to be renormalized.

B. On-shell and off-shell unitarity

As we have already anticipated, the solutions of the BSE must satisfy on-shell and off-shell unitarity. This is an important check for our amplitudes. This implies in turn conditions on the discontinuity ($\text{Disc}[f(s)] \equiv f(s + i\epsilon) - f(s - i\epsilon)$, $s > 4m^2$) of the functions $A(s)$, $B(s)$ and $C(s)$ for the $I = 0$ and $I = 2$ cases and $N(s)$ and $M(s)$ for the isovector one. Going through the unitarity conditions implicit in Eq. (2), we get a set of constraints which are compiled in Eqs. (A11) and (A12) of the Appendix A.

After a little of algebra, one can readily check that the discontinuity conditions of Eqs. (A11)-(A12) are satisfied by the off-shell amplitudes found in Subsect. III A. That guarantees that the solutions of the BSE found in that subsection satisfy both off-shell and on-shell unitarity.

For the on-shell case, elastic unitarity can be checked in a much simpler manner than that presented up to now. The on-shell amplitudes can be expressed in the following suggestive form which, as we will see, can be understood in terms of dispersion relations,

$$T_{IJ}^{-1}(s) = -\bar{I}_0(s) - C_{IJ} + \frac{1}{V_{IJ}(s)} \quad (25)$$

where C_{IJ} is a constant and the potentials are trivially read off from the on shell amplitudes in Eqs (18),(21) and (24). These potentials contain an infinite power series of $1/f^2$. In the on-shell limit, the unitarity condition for the partial waves is more easily expressed in terms of the inverse amplitude, for which the optical theorem for $s > 4m^2$ reads

$$\text{Im}T_{IJ}^{-1}(s + i\epsilon) = \frac{\lambda^{\frac{1}{2}}(s, m^2, m^2)}{16\pi s} = \frac{1}{16\pi} \sqrt{1 - \frac{4m^2}{s}} = -\text{Im}\bar{I}_0(s + i\epsilon) \quad (26)$$

thus, the on-shell amplitudes found in Subsect. III A for the several isospin-angular momentum channels trivially meet this requirement.

C. Crossing properties

On the mass-shell and at the lowest order in the chiral expansion presented in Subsect. III A, the Eq. (12) leads to

$$\begin{aligned} A_P(p, k) &= \frac{2}{3} (T_{00}(s) - T_{20}(s)) \\ B_P(p, k) &= T_{20}(s) - 3 \frac{u-t}{s-4m^2} T_{11}(s) \\ C_P(p, k) &= T_{20}(s) + 3 \frac{u-t}{s-4m^2} T_{11}(s) \end{aligned} \quad (27)$$

Obviously, the crossing conditions stated in Eq. (11) are not satisfied by the functions defined in Eq. (27), although they are fulfilled at lowest order in $1/f^2$. This is a common problem in all unitarization schemes. In the BSE the origin lies in the fact that the kernel of the equation, $\int d^4q \cdots \Delta(q_+) \Delta(q_-) \cdots$ breaks explicitly crossing, and given a potential V it only sums up all s -channel loop contributions generated by it. Thus this symmetry is only recovered when an exact *potential* V , containing t - and u -channel loop contributions, is used.

Actually, in our treatment of the channels $I = 0, 1, 2$ we require $3+2+3 = 8$ undetermined constants⁷, whereas crossing imposes to order $1/f^4$ only 4, namely $\bar{l}_{1,2,3,4}$. This is not as severe as one might think since we are summing up an infinite series in $1/f^2$. Nevertheless, we will show below how this information on crossing can be implemented at the level of partial waves.

⁷As we will discuss in the next subsection, a consistent renormalization program allows one to take the divergent integrals $I_0(4m^2), I_2(4m^2), I_4(4m^2)$ independent of each other in each isospin channel.

D. Renormalization of the amplitudes

To renormalize the on-shell amplitudes given in Eqs. (18),(21) and (24), or the corresponding ones for the case of off-shell scattering, we note that in the spirit of an EFT all possible counter-terms should be considered. This can be achieved in our case in a perturbative manner, making use of the formal expansion of the bare amplitude

$$T = V + VG_0V + VG_0VG_0V + \dots, \quad (28)$$

where G_0 is the two particle propagator. Thus, a counter-term series should be added to the bare amplitude such that the sum of both becomes finite. At each order in the perturbative expansion, the divergent part of the counter-term series is completely determined. However, the finite piece remains arbitrary. Our renormalization scheme is such that the renormalized amplitude can be cast, again, as in Eqs. (18),(21) and (24). This amounts in practice, to interpret the previously divergent quantities $I_{2n}(4m^2)$ as renormalized free parameters. After having renormalized, we add a superscript R to differentiate between the previously divergent, $I_{2n}(4m^2)$, and now finite quantities, $I_{2n}^R(4m^2)$. These parameters and therefore the renormalized amplitude can be expressed in terms of physical (measurable) magnitudes. In principle, these quantities should be understood in terms of the underlying QCD dynamics, but in practice it seems more convenient so far to fit $I_{2n}^R(4m^2)$ to the available data. The threshold properties of the amplitude (scattering length, effective range, etc..) can then be determined from them. Besides the pion properties m and f , at this order in the expansion we have 8 parameters. The appearance of 8 new parameters is not surprising because the highest divergence we find is quartic ($I_4(s)$) for the channels $I = 0$ and $I = 2$ and quadratic ($I_2(s)$) for the isovector channel and therefore to make the amplitudes convergent we need to perform 3+3+2 subtractions respectively. This situation is similar to what happens in standard ChPT where one needs to include low-energy parameters (\bar{l} 's). In fact, if t - and u - channel unitarity corrections are neglected, a comparison of our (now) finite amplitude, Eqs. (18),(21) and (24), to the $\mathcal{O}(p^4)$ $\pi\pi$ amplitude in terms of some of these \bar{l} 's becomes possible. Such a comparison will be discussed in the next subsection.

This renormalization scheme leads to a renormalized amplitude which does not derive from a renormalized Lagrangian. This is again closely linked to the violation of exact crossing symmetry, and it is detailed discussed in the Sect. A5 of the Appendix A.

E. Crossing Symmetry Restoration and Comparison with one loop ChPT

Our amplitudes contain undetermined parameters which, as stated previously outnumber those allowed by crossing symmetry at $\mathcal{O}(p^4)$. Nevertheless, by imposing suitable constraints on our parameters we can fulfill crossing symmetry approximately. We do this at the level of partial wave amplitudes. For completeness, we reproduce here a discussion from Ref. [12], where this issue was first addressed. At the lowest order in the chiral expansion proposed in this section, we approximate, in the scattering region $s > 4m^2$, the $\mathcal{O}(1/f^4)$ t - and u - channel unitarity corrections (function h_{IJ} in Eq. (B4) of the Appendix B) by a Taylor expansion around threshold to order $(s - 4m^2)^2$. At next order in our expansion (when the full $\mathcal{O}(p^4)$ -corrections are included both in the *potential* and in the pion propagator)

we will recover the full t - and u - channel unitarity logs at $\mathcal{O}(1/f^4)$, and at the next order ($\mathcal{O}(1/f^6)$), we will be approximating these logs by a Taylor expansion to order $(s - 4m^2)^3$. Thus, the analytical structure of the amplitude derived from the left hand cut is only recovered perturbatively. This is in common to other approaches (PR, DP, IAM \dots) fulfilling exact unitarity in the s -channel, as discussed in [4], [6], [17]. Thus, this approach violates crossing symmetry. At order $\mathcal{O}(1/f^4)$ our isoscalar s -, isovector p - and isotensor s -wave amplitudes are polynomials of degree two in the variable $(s - 4m^2)$, with a total of eight $(3+2+3)$ arbitrary coefficients $(I_{0,2,4}^{R,I=0}(4m^2), I_{0,2}^{R,I=1}(4m^2), I_{0,2,4}^{R,I=2}(4m^2))$, and there are no logarithmic corrections to account for t - and u -channel unitarity corrections. Far from the left hand cut, these latter corrections can be expanded in a Taylor series to order $(s - 4m^2)^2$, but in that case the one loop $SU(2)$ ChPT amplitudes can be cast as second order polynomials in the variable $(s - 4m^2)$, with a total of four $(\bar{l}_{1,2,3,4})$ arbitrary coefficients [16]. To restore, in this approximation, crossing symmetry in our amplitudes requires the existence of four constraints between our eight undetermined parameters. These relations can be found in Eq. (A15) in the Appendix A.

Once these constraints are implemented in our model, there exists a linear relation between our remaining four undetermined parameters $(I_{0,4}^{R,I=0}(4m^2), I_{0,2}^{R,I=1}(4m^2))$ and the most commonly used $\bar{l}_{1,2,3,4}$ parameters. Thus, all eight parameters $(I_{0,2,4}^{R,I=0,2}(4m^2), I_{0,2}^{R,I=1}(4m^2))$ can be expressed in terms of $\bar{l}_{1,2,3,4}$ (see Eq. (A16) of Appendix A).

F. Numerical results for $I = 0, 1, 2$

After the above discussion, it is clear that at this order we have four independent parameters $I_0^{R,I=0}$, $I_4^{R,I=0}$, $I_0^{R,I=1}$ and $I_2^{R,I=1}$ which can be determined either from a combined χ^2 -fit to the isoscalar and isotensor s - and isovector p -wave elastic $\pi\pi$ phase shifts or through, Eq. (A16), from the Gasser-Leutwyler or other estimates of the $\bar{l}_{1,2,3,4}$ low energy parameters. In a previous work, [12], we have already discussed the first procedure (χ^2 -fit) and thus we will follow here the second one. Therefore, we will try to address the following question: Does the lowest order of the off-shell BSE approach together with reasonable values for the $\bar{l}_{1,2,3,4}$ parameters describe the observed $\pi\pi$ phase-shifts in the intermediate energy region? To answer the question, we will consider two sets of parameters:

$$\begin{aligned} \text{set } \mathbf{A} : \bar{l}_1 &= -0.62 \pm 0.94, \bar{l}_2 = 6.28 \pm 0.48, \bar{l}_3 = 2.9 \pm 2.4, \bar{l}_4 = 4.4 \pm 0.3 \\ \text{set } \mathbf{B} : \bar{l}_1 &= -1.7 \pm 1.0, \bar{l}_2 = 6.1 \pm 0.5, \bar{l}_3 = 2.9 \pm 2.4, \bar{l}_4 = 4.4 \pm 0.3 \end{aligned} \quad (29)$$

In both sets \bar{l}_3 and \bar{l}_4 have been determined from the $SU(3)$ mass formulae and the scalar radius as suggested in [16] and in [18], respectively. On the other hand the values of $\bar{l}_{1,2}$ come from the analysis of Ref. [19] of the data on K_{l4} -decays (set \mathbf{A}) and from the combined study of K_{l4} -decays and $\pi\pi$ with some unitarization procedure (set \mathbf{B}) performed in Ref. [20].

Results are presented in Fig. 2 and in Table I. In the figure we show the prediction (solid lines) of the off-shell BSE approach, at lowest order, for the s - and p -wave $\pi\pi$ scattering phase-shifts for all isospin channels and for both sets \mathbf{A} (left panels) and \mathbf{B} (right panels) of the \bar{l} 's parameters. We assume Gauss distributed errors for the \bar{l} 's parameters and propagate those to the scattering phase shifts, effective range parameters, etc. . . by means of a Monte Carlo simulation. Central values for the phase-shifts have been computed using the central values of the \bar{l} 's parameters. Dashed lines in the plots are the 68% confidence limits.

As we see for both sets of constants, the simple approach presented here describes the isovector and isotensor channels up to energies above 1 GeV, whereas the isoscalar channel is well reproduced up to 0.8–0.9 GeV. In the latter case, and for these high energies, one should also include the mixing with the $K\bar{K}$ channel as pointed out recently in Refs. [8]–[9]. Regarding the deduced threshold parameters we find agreement with the measured values when both theoretical and experimental uncertainties are taken into account. Furthermore, both sets of parameters predict the existence of the ρ resonance⁸ in good agreement with the experimental data,

$$\begin{aligned} \text{set A : } m_\rho &= 770_{-60}^{+90} \text{ [MeV]}, \quad \Gamma_\rho = 180_{-50}^{+80} \text{ [MeV]} \\ \text{set B : } m_\rho &= 715_{-50}^{+70} \text{ [MeV]}, \quad \Gamma_\rho = 130_{-30}^{+60} \text{ [MeV]} \end{aligned} \tag{31}$$

In this way the “existence” of the ρ resonance can be regarded as a prediction of the BSE with ChPT and the parameters obtained from some low energy data. Favoring one of the considered sets of parameters, implies an assumption on the size of the $\mathcal{O}(p^6)$ contributions not included at this level of approximation. Finally, it is worth mentioning that the predicted parameters $I_n^R(4m^2)$, agree reasonably well with those fitted to $\pi\pi$ scattering data in Ref. [12].

	$J = I = 0$		$J = I = 1$		$J = 0, I = 2$	
	set A	set B	set A	set B	set A	set B
$-10^2 I_0^R(4m^2)$	3.1(4)	2.6(5)	9.8(14)	10.9(14)	6.6(6)	6.1(6)
$-10^3 I_2^R(4m^2)$	1.7(11)	3.0(12)	-77(7)	-83(8)	7.5(12)	8.4(12)
$-10^3 I_4^R(4m^2)$	3.0(12)	2.7(12)			2.1(5)	2.1(5)
$10^3 m^{2J+1} a_{IJ}$	225(7)	218(7)	39.5(11)	39.5(12)	-41.0(12)	-42.1(13)
$10^3 m^{2J+3} b_{IJ}$	308(20)	286(20)	7.3(14)	8.6(16)	-72.5(20)	-74.4(23)

TABLE I. Off-shell BSE approach parameters ($I_n^R(4m^2)$) obtained from both sets of \bar{l} 's parameters given in Eq. (29). $I_n^R(4m^2)$ are given in units of $(2m)^n$. We also give the threshold parameters a_{IJ} and b_{IJ} obtained from an expansion of the scattering amplitude [29], $\text{Re}T_{IJ} = -16\pi m(s/4 - m^2)^J [a_{IJ} + b_{IJ}(s/4 - m^2) + \dots]$ close to threshold. Errors have been propagated by means of a Monte Carlo simulation, they are given in brackets and affect to the last digit of the quoted quantities.

⁸We determine the position of the resonance, by assuming zero background and thus demanding the phase-shift, δ_{11} , to be $\pi/2$. Furthermore, we obtain the width of the resonance from

$$\frac{1}{\Gamma_\rho} = \frac{m_\rho}{(m_\rho^2 - s) \tan \delta_{11}(s)} = m_\rho \left. \frac{d\delta_{11}(s)}{ds} \right|_{s=m_\rho} = \frac{16\pi m_\rho^3}{\lambda^{\frac{1}{2}}(m_\rho^2, m^2, m^2)} \left. \frac{d\text{Re} T_{11}^{-1}(s)}{ds} \right|_{s=m_\rho} \tag{30}$$

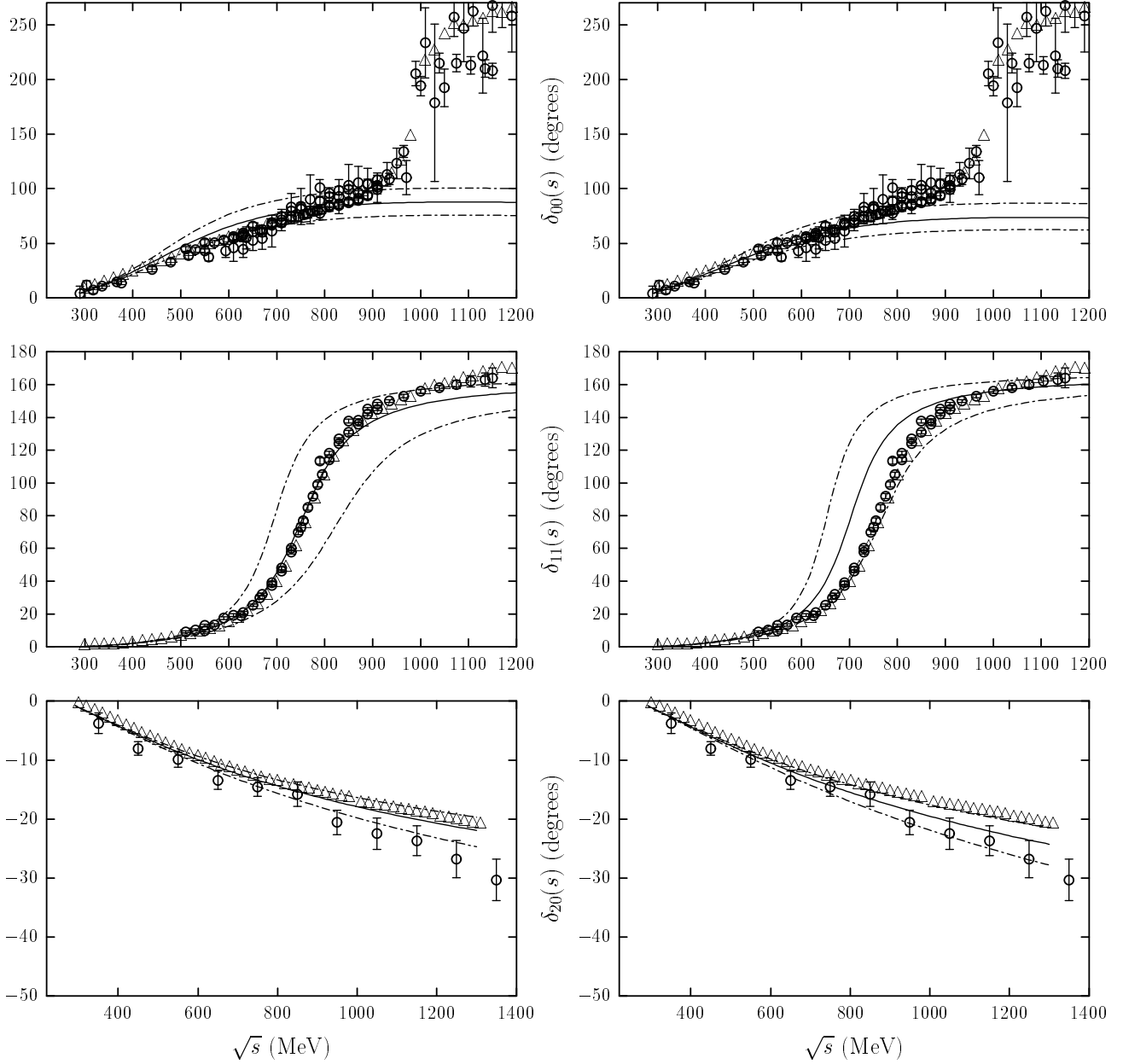


FIG. 2. Several $\pi\pi$ phase shifts as a function of the total CM energy \sqrt{s} for both sets of \bar{l} 's quoted in Eq. (29). Left (right) panels have been obtained with the set **A** (**B**) of parameters. Solid lines are the predictions of the off-shell BSE approach, at lowest order, for the different IJ -channels. Dashed lines are the 68% confidence limits. Top panels ($I = 0, J = 0$): circles stand for the experimental analysis of Refs. [21] - [26]. Middle panels ($I = 1, J = 1$): circles stand for the experimental analysis of Refs. [21] and [23]. Bottom panels ($I = 2, J = 0$): circles stand for the experimental analysis of Ref. [27]. In all plots the triangles are the Froggatt and Petersen phase-shifts (Ref. [28]) with no errors due to the lack of error estimates in the original analysis.

IV. ON-SHELL BSE SCHEME

As already recognized in previous work [12], it is very hard in practice to pursue the calculation of higher orders, within the off-shell scheme presented in the previous section. The difficulty lies on the non-locality of the four point Green-functions involved in the BSE in momentum space, and the subsequent and unavoidable renormalization. More specifically, to keep the full off-shell dependence of V and T in the BSE is the origin of most of the difficulties.

However, if we look at the amplitude in each isospin channel separately (Eqs. (18),(21) and (24)) it seems that the off-shellness can be ignored by simply renormalizing the parameters of the lowest order amplitude (f and m). The authors of Refs. [8] take advantage of this observation. Though, it is important to stress here, that this renormalization is different for each IJ -channel and therefore this procedure does not provide a satisfactory renormalization scheme.

In this section, we come up with a consistent and computationally feasible renormalization program where all off-shellness effects can be incorporated into a legitimate redefinition of the two particle irreducible amplitude, V , at all orders of the chiral expansion.

This new scheme allows us not only to describe the data but also to make predictions for some of the ChPT-low energy constants.

A. Renormalization of power divergences

Let us consider the iteration in the BSE of a renormalized potential, instead of the “bare” potential. Obviously, to define such a quantity requires a renormalization prescription⁹. This new viewpoint can only be taken, as we will see, because the divergence structure of the non-linear sigma model is such that, all non-logarithmic divergences can be absorbed by a suitable renormalization of the parameters of the Lagrangian. For completeness, we repeat here the argument given in Ref. [30] in a way that it can be easily applied to our case of interest. It is easier to consider first the chiral limit $m = 0$. The Lagrangian at lowest order is given by

$$\mathcal{L} = \frac{f^2}{4} \text{tr}(\partial^\mu U^\dagger \partial_\mu U) \quad (32)$$

with U a dimensionless unitarity matrix, involving the Goldstone fields, which transforms linearly under the chiral group. Thus, the necessary counter-terms to cancel L loops are suppressed by the power $f^{2(1-L)}$. Let Λ be a chiral invariant regulator with dimension of energy and D the dimension of a counter-term which appears at L loops. Since the U field is dimensionless, D simply counts the number of derivatives. The operator appearing in the counter-term Lagrangian should have dimension 4, thus we have

$$D = 2 + 2L - r \quad (33)$$

⁹In the following we will assume a mass independent regularization scheme, such as e.g. dimensional regularization. The reason for doing this is that it preserves chiral symmetry.

with r the number of powers of the regulator Λ which accompany this counter-term in the Lagrangian (degree of divergence). If we denote the counter-terms in the schematic way

$$\mathcal{L}_{\text{ct}} = \sum_{L=0}^{\infty} f^{2(1-L)} \sum_i c_{i,r}^L \sum_{r=0}^{2L} \Lambda^r \langle \partial^{2+2L-r} \rangle_i \quad (34)$$

where $\langle \partial^D \rangle_i$ denotes a set of chiral invariant linear independent operators made out of the matrix U and comprising D derivatives and $c_{i,r}^L$ are suitable dimensionless coefficients. We see that at L loops the only new structures are those corresponding to Λ^0 ($r = 0$) which in actual calculations corresponds to logarithmic divergences. Higher powers in Λ generate structures which were already present at $L - 1$ loops. For instance, let us consider the one-loop correction, by construction it is down respect to the leading order by two powers of f , i.e., the corresponding counter-terms in the Lagrangian will be made out of chiral invariant operators constructed by means of derivatives of the dimensionless U matrix, defined above, and any of them will be multiplied by an overall factor f^0 . In addition, the total energy dimension of the counter-terms has to be four. Hence, only terms with two and four derivatives¹⁰ might appear. To get the proper dimensions, these terms will have to be multiplied by Λ^2 and $\Lambda^0 \ln \Lambda$ respectively. Thus, the quadratic divergence, first term, is a renormalization of the leading kinetic energy piece (Eq. (32)). Besides, to renormalize the logarithmic divergence, one has to add new counter-terms, not present in the original Lagrangian (Eq. (32)). For higher loops, the argument can be easily generalized, see for more details Ref. [30].

This result is very important because it means that all but the logarithmic divergences can effectively be ignored. An efficient scheme which accomplishes this property is dimensional regularization, since

$$\int \frac{d^4 q}{(2\pi)^4} (q^2)^n = 0 \quad n = -1, 0, 1, \dots \quad (35)$$

This argument can be extended away from the chiral limit, although in this case new terms appear which vanish in the limit $m^2 \rightarrow 0$. The conclusion is again the same. If every possible counter-term compatible with chiral symmetry is written down, all but the logarithmic divergent pieces can be ignored.

The above discussion means that when renormalizing the BSE, we may set to zero (at a given renormalization point) all power divergent integrals which appeared in Sect. III. This is because they only amount to a renormalization of the undetermined parameters of the higher order terms of the Lagrangian. The power of this result is a direct consequence of the symmetry, the derivative coupling of the pion interactions and the fact that in ChPT there is an infinite tower of operators. In a sense this is only true for the exact theory with an infinite set of counter-terms, it is to say when we iterate by means of the BSE a “renormalized” two particle irreducible amplitude, V , with an infinite number of terms.

¹⁰Note that an odd-number of derivatives are forbidden by parity conservation and the only chirally invariant operator with zero derivatives is $\text{tr}(UU^\dagger) = 2$, an irrelevant constant.

To keep all power divergences and not only the logarithmic ones and simultaneously iterate the most general two particle irreducible amplitude leads to redundant combinations of undetermined parameters. For instance, to include in the potential the tree $\mathcal{O}(p^4)$ Lagrangian (\bar{l} 's) and keep the power (non logarithmic) divergences produced by the loops made out of the $\mathcal{O}(p^2)$ pieces of the Lagrangian produces redundant contributions at $\mathcal{O}(p^4)$ (Eq. (A16) illustrates clearly the point). These redundancies also appear at higher orders if higher order tree Lagrangian terms are also included in the potential, V .

B. Off-shell versus on-shell

Let us consider the BSE in the case of $\pi\pi$ scattering. The isospin amplitudes satisfy the symmetry properties given in Eqs. (6) and (10). Thus, they admit the following expansion

$$T_P^I(p, k) = \sum_{N_1} \sum_{N_2} \sum_{\mu_1 \mu_2 \dots} T_{\mu_1 \dots \mu_{N_1}; \nu_1 \dots \nu_{N_2}}^I [P] k^{\mu_1} \dots k^{\mu_{N_1}} p^{\nu_1} \dots p^{\nu_{N_2}} \quad (36)$$

where $T_{\mu_1 \dots \mu_{N_1}; \nu_1 \dots \nu_{N_2}}^I [P] = T_{\nu_1 \dots \nu_{N_2}; \mu_1 \dots \mu_{N_1}} [P]$ and N_1 and N_2 run only over even (odd) natural numbers for the $I = 0, 2$ ($I = 1$) isospin channel. In short hand notation we may write

$$T_P^I(p, k) = \sum_{(\mu)(\nu)} T_{(\mu)(\nu)}^I [P] k^{(\mu)} p^{(\nu)} \quad (37)$$

Inserting this ansatz in the BSE, for simplicity let us consider first only those contributions where the free meson propagators ($\Delta^{(0)}$) are used, we get

$$T_{(\mu)(\nu)}^I [P] = V_{(\mu)(\nu)}^I [P] + i \sum_{(\alpha)(\beta)} T_{(\mu)(\alpha)}^I [P] \int \frac{d^4 q}{(2\pi)^4} q^{(\alpha)} q^{(\beta)} \Delta^{(0)}(q_+) \Delta^{(0)}(q_-) V_{(\beta)(\nu)}^I [P] \quad (38)$$

Due to parity the number of indices in (α) and in (β) ought to be either both even or both odd. Thus, we are led to consider the integral

$$I_{2k}^{\mu_1 \dots \mu_{2n}} [P] := i \int \frac{d^4 q}{(2\pi)^4} q^{2k} q^{\mu_1} \dots q^{\mu_{2n}} \Delta^{(0)}(q_+) \Delta^{(0)}(q_-) \quad (39)$$

If we contract the former expression with P^{μ_1} we get, using that

$$2P \cdot q = \left(\frac{1}{\Delta^{(0)}(q_+)} - \frac{1}{\Delta^{(0)}(q_-)} \right), \quad (40)$$

the identity

$$P_{\mu_1} I_{2k}^{\mu_1 \dots \mu_{2n}} [P] = -i \int \frac{d^4 q}{(2\pi)^4} q^{2k} q^{\mu_2} \dots q^{\mu_{2n}} \Delta^{(0)}(q_+) \quad (41)$$

Shifting the integration variable

$$\begin{aligned} P_{\mu_1} I_{2k}^{\mu_1 \dots \mu_N} [P] &= -i \int \frac{d^4 q}{(2\pi)^4} \Delta^{(0)}(q) \left((q^2 - m^2) + \left(\frac{s}{4} + m^2 \right) - q \cdot P \right)^k \\ &\quad \times (q - P/2)^{\mu_2} \dots (q - P/2)^{\mu_{2n}} \end{aligned} \quad (42)$$

which corresponds to quadratic and higher divergences. As we have said before, only the logarithmic divergences should be taken into account since higher order divergences can be absorbed as redefinition of the renormalized parameters of the higher order terms of the Lagrangian. Thus, we would get that, up to these non-logarithmic divergences, the integral is transverse, i.e. when contracted with some P^μ becomes zero. The transverse part can be calculated to give

$$I_{2k}^{\mu_1 \dots \mu_{2n}}[P] := C_{nk}(s) \left[\left(g^{\mu_1 \mu_2} - \frac{P^{\mu_1} P^{\mu_2}}{s} \right) \dots \left(g^{\mu_{2n-1} \mu_{2n}} - \frac{P^{\mu_{2n-1}} P^{\mu_{2n}}}{s} \right) \right. \\ \left. + \text{Permutations} \right] + \text{P.D.} \quad (43)$$

where $C_{nk}(s)$ is a function¹¹ of s and P. D. means power divergences. Let us study now the integral $I_{2n}(s)$ and use that

$$q^2 = \left(m^2 - \frac{s}{4} \right) + \frac{1}{2} \left(\Delta^{(0)}(q_+)^{-1} + \Delta^{(0)}(q_-)^{-1} \right) \quad (45)$$

then we get

$$I_{2n}(s) = \left(m^2 - \frac{s}{4} \right) I_{2n-2}(s) + i \int \frac{d^4 q}{(2\pi)^4} \Delta^{(0)}(q) q_+^{2n-2} \quad (46)$$

Again, the second term corresponds to power divergences. Applying this formula n times we get

$$I_{2n}(s) = \left(m^2 - \frac{s}{4} \right)^n I_0(s) + \text{P.D.} \quad (47)$$

All this discussion means that under the integral sign we may set $q^2 = m^2 - s/4$ and $P \cdot q = 0$ up to non-logarithmic divergences, i.e.

$$i \int \frac{d^4 q}{(2\pi)^4} F(q^2; P \cdot q) \Delta^{(0)}(q_+) \Delta^{(0)}(q_-) = F\left(m^2 - \frac{s}{4}; 0\right) I_0(s) + \text{P.D.} \quad (48)$$

Up to now we have considered the bare (free) meson propagator $\Delta^{(0)}$. If we have the full renormalized propagator

$$\Delta(q) = \left(q^2 - m^2 - \Pi(q^2) \right)^{-1} \quad (49)$$

where $\Pi(q^2)$ is the meson self-energy with the on-shell renormalization conditions

$$\Pi(m^2) = 0, \quad \Pi'(m^2) = 0 \quad (50)$$

¹¹It can be shown that

$$C_{nk}(s) = \frac{1}{(2n+1)!!} I_{2n+2k}(s). \quad (44)$$

then we have the Laurent expansion around the mass pole, $q^2 = m^2$,

$$\Delta(q) = \frac{1}{q^2 - m^2} + \frac{1}{2}\Pi''(m^2) + \dots \quad (51)$$

The non-pole terms of the expansion generate, when applied to the kernel of the BSE, power divergences. Therefore, Eq. (48) remains valid also when the full renormalized propagator $\Delta(q)$ is used.

In conclusion, the off-shellness of the BSE kernel leads to power divergences which have to be renormalized by a suitable Lagrangian of counter-terms (for instance the bare $l's$ -Lagrangian pieces at order $\mathcal{O}(p^4)$), leaving the resulting finite parts as undetermined parameters of the EFT. Thus, if we iterate a renormalized potential we should ignore the power divergences and therefore ignore the off-shell behavior within the BSE and then solve

$$T_P^I(p, k) = V_P^I(p, k) + i \int \frac{d^4q}{(2\pi)^4} T_P^I(\bar{q}, k) \Delta(q_+) \Delta(q_-) V_P^I(p, \bar{q}) \quad (52)$$

with

$$\bar{q}^\mu \bar{q}^\nu = \frac{m^2 - s/4}{q^2 - (P \cdot q)^2/s} \left(q^\mu - P^\mu \frac{(P \cdot q)}{s} \right) \left(q^\nu - P^\nu \frac{(P \cdot q)}{s} \right); \quad \bar{q}^2 = m^2 - s/4 \quad (53)$$

Thus, given the exact two particle irreducible amplitude, potential V^I , the solution of Eq. (1), in a given isospin channel, and that of Eq. (52) are equivalent. This important result will allow us in the next subsection to find an exact solution of the BSE given an exact two particle irreducible amplitude, V . It also might justify the method used in Refs. [8], [9] where the off-shell behavior of the Lippmann-Schwinger equation is totally ignored.

C. Partial wave expansion

We now show how the BSE can be diagonalized within this on-shell scheme for $s > 0$. To this end we consider the following off-shell ‘‘partial wave’’ expansions for $T_P^I(p, k)$ and $V_P^I(p, k)$

$$T_P^I(p, k) = \sum_{J=0}^{\infty} (2J+1) T_{IJ}(p^2, P \cdot p; k^2, P \cdot k) P_J(\cos\theta_{k,p}) \quad (54)$$

and a similar one for $V_P^I(p, k)$. The ‘‘angle’’ $\theta_{k,p}$ is given by

$$\cos\theta_{k,p} := \frac{-p \cdot k + (P \cdot p)(P \cdot k)/s}{[(P \cdot p)^2/s - p^2]^{\frac{1}{2}} [(P \cdot k)^2/s - k^2]^{\frac{1}{2}}} \quad (55)$$

and it reduces to the scattering angle in the CM system for mesons on the mass shell. For $s > 0$, the Legendre polynomials satisfy a orthogonality relation of the form

$$i \int \frac{d^4q}{(2\pi)^4} \Delta(q_+) \Delta(q_-) P_J(\cos\theta_{k,\bar{q}}) P_{J'}(\cos\theta_{\bar{q},p}) = \delta_{JJ'} \frac{P_J(\cos\theta_{k,p})}{2J+1} I_0(s) \quad (56)$$

which is the generalization of the usual one. Plugging the partial wave expansions of Eq. (54) for the amplitude and potential in Eq. (52) we get¹²

$$T_{IJ}(p^2, P \cdot p; k^2, P \cdot k) = V_{IJ}(p^2, P \cdot p; k^2, P \cdot k) + T_{IJ}(m^2 - \frac{s}{4}, 0; k^2, P \cdot k) I_0(s) V_{IJ}(p^2, P \cdot p; m^2 - \frac{s}{4}, 0) \quad (57)$$

To solve this equation, we set the variable p on-shell, and get for the half off-shell amplitude

$$T_{IJ}(m^2 - \frac{s}{4}, 0; k^2, P \cdot k)^{-1} = -I_0(s) + V_{IJ}(m^2 - \frac{s}{4}, 0; k^2, P \cdot k)^{-1} \quad (58)$$

Likewise, for the full on-shell amplitude we get

$$T_{IJ}(m^2 - \frac{s}{4}, 0; m^2 - \frac{s}{4}, 0)^{-1} := T_{IJ}(s)^{-1} = -I_0(s) + V_{IJ}(s)^{-1} \quad (59)$$

where $V_{IJ}(s) = V_{IJ}(m^2 - s/4, 0; m^2 - s/4, 0)$. Choosing the subtraction point s_0 we have a finite on-shell amplitude

$$T_{IJ}(s)^{-1} - T_{IJ}(s_0)^{-1} = -(I_0(s) - I_0(s_0)) + V_{IJ}(s)^{-1} - V_{IJ}(s_0)^{-1} \quad (60)$$

A finite (renormalized) inverse half-off-shell can now be obtained from the finite (renormalized) on-shell amplitude

$$\begin{aligned} T_{IJ}(m^2 - \frac{s}{4}, 0; k^2, P \cdot k)^{-1} &= T_{IJ}(s)^{-1} + V_{IJ}(m^2 - \frac{s}{4}, 0; k^2, P \cdot k)^{-1} - V_{IJ}(s)^{-1} \\ &= T_{IJ}(s_0)^{-1} - (I_0(s) - I_0(s_0)) \\ &\quad + \left(V_{IJ}(m^2 - \frac{s}{4}, 0; k^2, P \cdot k)^{-1} - V_{IJ}(s_0)^{-1} \right) \end{aligned} \quad (61)$$

Note that once we have the half off shell amplitude we might, through Eq. (57), get the full off-shell one. The idea of reconstructing the full off-shell amplitude from both the on- and half off-shell amplitudes was first suggested in Ref. [31], where a dispersion relation inspired treatment of the BSE, with certain approximations, was undertaken.

D. Off-shell unitarity

The off-shell unitarity condition becomes particularly simple in terms of partial wave amplitudes. Taking into account Eq. (2), that in this equation and due to the on-shell delta functions q^μ can be replaced by \bar{q}^μ in the arguments of the T -matrices, and taking discontinuities in Eq. (56) one can see that in terms of partial waves, off-shell unitarity reads:

$$\begin{aligned} T_{IJ}(p^2, P \cdot p; k^2, P \cdot k) - T_{IJ}^*(k^2, P \cdot k; p^2, P \cdot p) \\ = T_{IJ}(m^2 - \frac{s}{4}, 0; k^2, P \cdot k) \text{Disc}[I_0(s)] T_{IJ}^*(m^2 - \frac{s}{4}, 0; p^2, P \cdot p) \end{aligned} \quad (62)$$

¹² We preserve the ordering in multiplying the expressions in a way that the generalization to the coupled channel case becomes evident.

A solution of the form in Eq. (57) automatically satisfies¹³ the off-shell unitarity condition of Eq. (62). This property is maintained even if an approximation to the exact potential in Eq. (57) is made.

E. Approximations to the Potential

Given the most general two particle irreducible renormalized amplitude, $V_P(p, k)$, compatible with the chiral symmetry for on-shell scattering, Eq. (60) provides an exact T -matrix for the scattering of two pions on the mass shell, for any IJ -channel. Eq. (60) can be rewritten in the following form

$$T_{IJ}(s)^{-1} + \bar{I}_0(s) - V_{IJ}(s)^{-1} = T_{IJ}(s_0)^{-1} + \bar{I}_0(s_0) - V_{IJ}(s_0)^{-1} = -C_{IJ} \quad (64)$$

where C_{IJ} should be a constant, independent of s . Thus we have

$$T_{IJ}(s)^{-1} = -\bar{I}_0(s) - C_{IJ} + V_{IJ}(s)^{-1} \quad (65)$$

or defining $W_{IJ}(s, C_{IJ})^{-1} = -C_{IJ} + V_{IJ}(s)^{-1}$ the above equation can be written

$$T_{IJ}(s)^{-1} = -\bar{I}_0(s) + W_{IJ}(s)^{-1} \quad (66)$$

The functions $\bar{I}_0(s)$ and $W_{IJ}(s)$ or $V_{IJ}(s)$ account for the right and left hand cuts [32] respectively of the inverse amplitude $T_{IJ}(s)^{-1}$. The function $W_{IJ}(s)$, or equivalently $V_{IJ}(s)$, is a meromorphic function in $\mathbb{C} - \mathbb{R}^-$, is real through the unitarity cut and contains the essential dynamics of the process. Thus, analyticity considerations ([32]) tell us that the scattering amplitude should be given by

$$T_{IJ}^{-1}(s) = -\bar{I}_0(s) + \frac{P^{IJ}(s)}{Q^{IJ}(s)} \quad (67)$$

where $P^{IJ}(s)$ and $Q^{IJ}(s)$ are analytical functions of the complex variable $s \in \mathbb{C} - \mathbb{R}^-$. A systematic approximation to the above formula can be obtained by a *Pade* approximant to the *inverse potential*, although not exactly in the form proposed in Ref. [2],

$$T_{IJ}^{-1}(s) = -\bar{I}_0(s) + \frac{P_n^{IJ}(s - 4m^2)}{Q_k^{IJ}(s - 4m^2)} \quad (68)$$

¹³To prove this statement it is advantageous to note that above the unitarity cut, where the potential V is hermitian,

$$\begin{aligned} T_{IJ}^*(k^2, P \cdot k; p^2, P \cdot p) &= V_{IJ}(p^2, P \cdot p; k^2, P \cdot k) \\ &+ V_{IJ}(m^2 - \frac{s}{4}, 0; k^2, P \cdot k) I_0^*(s) T_{IJ}^*(m^2 - \frac{s}{4}, 0; p^2, P \cdot p) \end{aligned} \quad (63)$$

where $P_n^{IJ}(x)$ and $Q_k^{IJ}(x)$ are polynomials¹⁴ of order n and k with real coefficients. Crossing symmetry relates some of the coefficients of the polynomials for different IJ -channels, but can not determine all of them and most of these coefficients have to be fitted to the data or, if possible, be understood in terms of the underlying QCD dynamics. This type of *Pade* approach was already suggested in Ref. [12]. Actually, the results of the off-shell scheme presented in Sect. III are just *Pade* approximants of the type $[n, k] = [1, 1]$ in Eq. (68).

A different approach would be to propose an effective range expansion for the function $W_{IJ}(s)$, namely

$$W_{IJ}(s) = \sum_{n=0}^{\infty} \alpha_{IJ}^{(n)} (s - 4m^2)^{n+J} \quad (69)$$

or a chiral expansion of the type

$$W_{IJ}(s) = \sum_{n=1}^{\infty} \beta_{IJ}^{(n)} (s/m^2) \left(\frac{m^2}{f^2} \right)^n \quad (70)$$

where the $\beta_{IJ}^{(n)}(s/m^2)$ functions are made of polynomials and logarithms (chiral logs). As we explain below, the ability to accommodate resonances reduces the applicability of these approximations (Eqs. (69) and (70)) in practice.

As discussed above, the function $W_{IJ}(s)$ is real in the elastic region of scattering. Obviously, the zeros of $T_{IJ}(s)$ and $W_{IJ}(s)$ coincide in position and order¹⁵. For real s above the two particle threshold, zeros could appear for a phase shift $\delta_{IJ}(s) = n\pi$, $n \in \mathbb{N}$, in which case a resonance has already appeared at a lower energy. For the present discussion we can ignore these zeros. The first resonance would appear at $\sqrt{s} = m_R$ for which $\delta_{IJ}(m_R) = \pi/2$ and hence $\text{Re}T_{IJ}^{-1}(m_R) = 0$, i.e., $-\text{Re}\bar{I}_0(m_R) + W_{IJ}^{-1}(m_R) = 0$, but $\text{Re}\bar{I}_0(s) > 0$, so a necessary condition for the existence of the resonance is that $W_{IJ}(m_R) > 0$. On the other hand, the sign of $W_{IJ}(s)$ is fixed between threshold and the zero at $\delta_{IJ}(s) = n\pi$. It turns out that due to chiral symmetry the functions W_{11} and W_{00} are always negative for $\pi\pi$ scattering so the existence of the σ and ρ resonances can not be understood.

The above argument overlooks the fact that the change in sign of W_{IJ} may be also due to the appearance of a pole at $s = s_p$, which does not produce a pole in T_{IJ} , since $T_{IJ}(s_p) = -1/\bar{I}_0(s_p)$. The problem is that if that W_{IJ} has to diverge before we come to the resonance, how can an approximate expansion, of the type in Eqs. (69) and (70), for W_{IJ} produce this pole, and if so how could the expansion be reliable at this energy region? To get the proper perspective we show in Fig. 3 the inverse of the function W_{11} (circles in the middle plot) for $\pi\pi$ scattering extracted from experiment through Eq. (66). The presence of a pole (zero in the inverse function) in W_{11} is evident since the ρ resonance exists!

We suggest to use Eq. (65) rather than Eq. (66) with the inclusion of a further unknown parameter C_{IJ} , because in contrast to the function W_{IJ} , the potential V_{IJ} can be approximated by expansions of the type given in Eqs. (69) and (70). It is clear that with the new

¹⁴Note that the first non-vanishing coefficient in Q_n corresponds to the power $(s - 4m^2)^J$.

¹⁵ In $\pi\pi$ scattering, the location of one zero for each I and J is known approximately (see e.g. Ref. [33]) in the limit of small s and m and are called Adler zeros.

constant C_{IJ} , $\text{Re}T_{IJ}^{-1}$ can vanish without requiring a change of sign in the new potential $V_{IJ}(s)$. Thus, $V_{IJ}(s)$ can be kept small as to make the use of perturbation theory credible. The effect of this constant on the potential extracted from the data can be seen in Fig. 3 for several particular values.

After this discussion, it seems reasonable to propose some kind of expansion (effective range, chiral,...) for the potential $V_{IJ}(s)$ rather than for the function $W_{IJ}(s)$. The role played by the renormalization constant C_{IJ} will have to be analyzed. Thus, in the next subsection we use a chiral expansion of the type

$$V_{IJ}(s) = \sum_{n=1}^{\infty} V_{IJ}^{(2n)}(s/m^2) \left(\frac{m^2}{f^2}\right)^n \quad (71)$$

where the $^{(2n)}V_{IJ}(s/m^2)$ functions are made of polynomials and logarithms (chiral logs). In this way we will be able to determine the higher order terms of the ChPT Lagrangian not only from the threshold data, as it is usually done in the literature, but from a combined study of both the threshold and the low-lying resonance region.

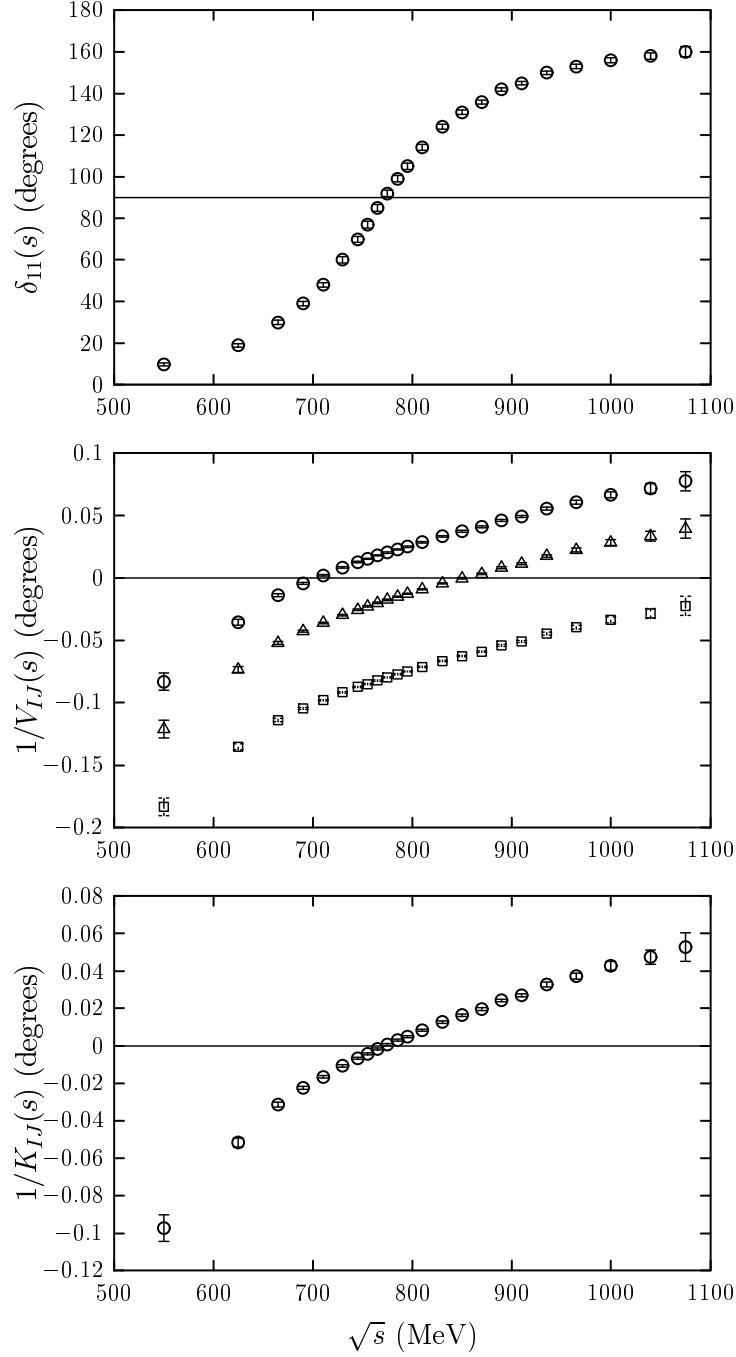


FIG. 3. Experimental isovector p -wave phase shifts (top panel), inverse of the functions $V_{11}(s)$ (middle panel) and $K_{11}(s)$ (bottom panel) as a function of the total CM energy \sqrt{s} . Phase shifts are taken from the experimental analysis of Ref. [21] and $V_{11}^{-1}(s)$ is determined through Eq. (65) from the data of the top panel and using three values of the constant C_{11} : 0 ($V_{11} = W_{11}$), -0.1 (as suggested by the results of Table I) and -0.038 (as suggested by the formula $[\log(m/\mu) - 1]/8\pi^2$ with a scale μ of the order of 1 GeV, see Eq. (116)), which are represented by circles, squares and triangles respectively. Finally, K_{11} is also determined from the data of the top panel through Eq. (120).

F. Chiral expansion of the on-shell potential

The chiral expansion of the $\pi\pi$ elastic scattering amplitude reads

$$T_{IJ}(s) = T_{IJ}^{(2)}(s)/f^2 + T_{IJ}^{(4)}(s)/f^4 + T_{IJ}^{(6)}(s)/f^6 + \dots \quad (72)$$

where $T_{IJ}^{(2)}(s)$, $T_{IJ}^{(4)}(s)$ and $T_{IJ}^{(6)}(s)$ can be obtained from Refs. [33], [16] and [34]– [35] respectively. For the sake of completeness we give in the Appendix B the leading and next-to-leading orders.

If we consider the similar expansion for the potential V_{IJ} given in Eq. (71) and expand in power series of m^2/f^2 the amplitude given in Eq. (65) we get

$$\begin{aligned} T_{IJ} = & \frac{m^2}{f^2} V_{IJ}^{(2)} + \frac{m^4}{f^4} \left(V_{IJ}^{(4)} + (\bar{I}_0 + C_{IJ}) [V_{IJ}^{(2)}]^2 \right) \\ & + \frac{m^6}{f^6} \left(V_{IJ}^{(6)} + 2(\bar{I}_0 + C_{IJ}) V_{IJ}^{(4)} V_{IJ}^{(2)} + (\bar{I}_0 + C_{IJ})^2 [V_{IJ}^{(2)}]^3 \right) \dots \end{aligned} \quad (73)$$

Matching the expansions of Eqs. (72) and (73) we find

$$\begin{aligned} m^2 V_{IJ}^{(2)} &= T_{IJ}^{(2)} \\ m^4 V_{IJ}^{(4)} &= T_{IJ}^{(4)} - (\bar{I}_0 + C_{IJ}) [T_{IJ}^{(2)}]^2 = \tau_{IJ}^{(4)} - C_{IJ} [T_{IJ}^{(2)}]^2 \\ &\dots \end{aligned} \quad (74)$$

with $\tau_{IJ}^{(4)}$ defined in Eq. (B2). From the unitarity requirement

$$\text{Im}T_{IJ}^{(4)}(s) = -\frac{1}{16\pi} \sqrt{1 - \frac{4m^2}{s}} [T_{IJ}^{(2)}(s)]^2, \quad s > 4m^2 \quad (75)$$

and thus, we see that $V_{IJ}^{(4)}$ is real above the unitarity cut, as it should be.

Thus, in this expansion we get the following formula for the inverse scattering amplitude

$$\begin{aligned} T_{IJ}^{-1}(s) &= -\bar{I}_0(s) - C_{IJ} + \frac{1}{T_{IJ}^{(2)}(s)/f^2 + T_{IJ}^{(4)}(s)/f^4 - (\bar{I}_0(s) + C_{IJ}) [T_{IJ}^{(2)}(s)]^2/f^4 + \dots} \\ &= -\bar{I}_0(s) - C_{IJ} + \frac{1}{T_{IJ}^{(2)}(s)/f^2 + \tau_{IJ}^{(4)}(s)/f^4 - C_{IJ} [T_{IJ}^{(2)}(s)]^2/f^4 + \dots} \end{aligned} \quad (76)$$

Notice that reproducing ChPT to some order means neglecting higher order terms in s/f^2 and m^2/f^2 , which is not the same as going to low energies. With the constant C_{IJ} we may be able to improve the low energy behavior of the amplitude. Obviously, the *exact* amplitude $T_{IJ}(s)$ is independent on the value of the constant C_{IJ} , but the smallness of $V_{IJ}(s)$ depends on C_{IJ} . Ideally, with an appropriated choice of C_{IJ} , $V_{IJ}(s)$ would be, in a determined region of energies, as small as to make the use of perturbation theory credible and simultaneously fit the data.

Any unitarization scheme which reproduces ChPT to some order, is necessarily generating all higher orders. For instance, if we truncate the expansion at fourth order we would “predict” a sixth order

$$\bar{T}_{IJ}^{(6)} = 2(\bar{I}_0 + C_{IJ}) \left(\tau_{IJ}^{(4)} - C_{IJ} [T_{IJ}^{(2)}]^2 \right) T_{IJ}^{(2)} + (\bar{I}_0 + C_{IJ})^2 [T_{IJ}^{(2)}]^3 \quad (77)$$

and so on.

Finally, we would like to point out that within this on-shell scheme crossing symmetry is restored more efficiently than within the off-shell scheme exposed in Sect. III. Thus, for instance, if we truncate the expansion at fourth order and neglect terms of order $1/f^6$, crossing symmetry is exactly restored at all orders in the expansion ($s - 4m^2$), whereas in the off-shell scheme this is only true if the u - and t - unitarity corrections are Taylor expanded around $4m^2$ and only the leading terms in the expansions are kept.

G. Form Factors

The interest in determining the half-off shell amplitudes lies upon their usefulness in computing vertex functions. Let $\Gamma_P(p, k)$ be the irreducible three-point function, connecting the two meson state to the corresponding current. The BSE for this vertex function, Fig. 4, is then

$$F_P^{ab}(k) = \Gamma_P^{ab}(k) + \frac{1}{2} \sum_{cd} i \int \frac{d^4 q}{(2\pi)^4} T_P(q, k)_{cd;ab} \Delta(q_+) \Delta(q_-) \Gamma_P^{cd}(q) \quad (78)$$

and using the BSE we get alternatively

$$F_P^{ab}(k) = \Gamma_P^{ab}(k) + \frac{1}{2} \sum_{cd} i \int \frac{d^4 q}{(2\pi)^4} V_P(q, k)_{cd;ab} \Delta(q_+) \Delta(q_-) F_P^{cd}(q) \quad (79)$$

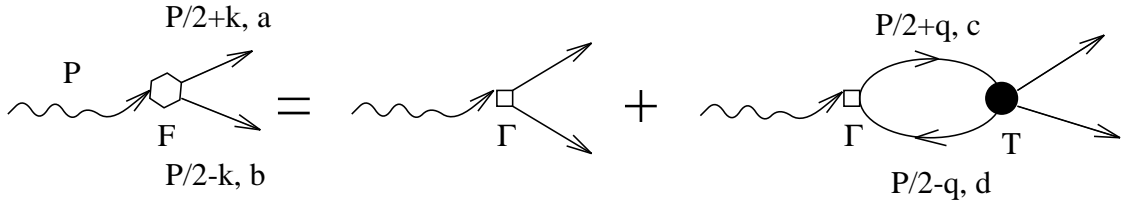


FIG. 4. Diagrammatic representation of the BSE type equation used to compute vertex functions. It is also sketched the used kinematics and a, b, c, d are isospin indices.

In operator language we have $F = \Gamma + VG_0F = \Gamma + TG_0\Gamma$, with G_0 the two particle propagator. The discontinuity in F is then given by the discontinuities of the scattering amplitude T and the two particle propagator G_0 .

The off-shellness of the kernel of Eq. (78) leads to power divergences which have to be renormalized by appropriate Lagrangian counter-terms. The resulting finite parts are undetermined parameters of the EFT (for instance \bar{l}_6 , at order $\mathcal{O}(p^4)$, for the vector vertex). The situation is similar to that discussed in Subsect. IV A for the scattering amplitude, and thus if we iterate a renormalized irreducible three-point function, Γ , we should ignore the power divergences and therefore ignore the off-shell behavior of the kernel of Eq. (78) and then solve

$$F_P^{ab}(k) = \Gamma_P^{ab}(k) + \frac{1}{2} \sum_{cd} i \int \frac{d^4 q}{(2\pi)^4} T_P(\bar{q}, k)_{cd;ab} \Delta(q_+) \Delta(q_-) \Gamma_P^{cd}(\bar{q}) \quad (80)$$

with \bar{q} given in Eq. (53). The above equation involves the half-off or on-shell amplitudes for off-shell ($k^2 \neq m^2$) or on-shell ($k^2 = m^2$) vertex functions respectively.

1. Vector form factor

The vector form factor, $F_V(s)$, is defined by

$$\left\langle \pi^a(P/2 + k) \pi^b(P/2 - k) \left| \frac{1}{2} (\bar{u} \gamma_\mu u - \bar{d} \gamma_\mu d) \right| 0 \right\rangle = -2i F_V(s) \epsilon_{ab3} k_\mu \quad (81)$$

where $s = P^2$, a, b are Cartesian isospin indices, u, d and γ_μ are Dirac fields, with flavor ‘‘up’’ and ‘‘down’’, and matrices respectively. For on-shell mesons, $k \cdot P = 0$ and then the vector current $\frac{1}{2} (\bar{u} \gamma_\mu u - \bar{d} \gamma_\mu d)$ is conserved as demanded by gauge invariance. The vector form factor is an isovector, and we calculate here its $I_z = 0$ component, thus the sum over isospin in Eq. (80) selects the $I = 1$ channel. Then, we have

$$F_V(s) k^\mu = \Gamma_V(s) k^\mu + i \Gamma_V(s) \int \frac{d^4 q}{(2\pi)^4} T_P^1(\bar{q}, k) \Delta(q_+) \Delta(q_-) \bar{q}^\mu \quad (82)$$

with $\Gamma_V(s)$ related with the irreducible vector three-point vertex by means of

$$\Gamma_P^{ab}(k) = -2i \Gamma_V(s) \epsilon_{ab3} k_\mu \quad (83)$$

Using a partial-wave expansion for $T_P^1(\bar{q}, k)$ (Eq. (54)) and the orthogonality relation given in Eq. (56) the integral in Eq. (82) can be performed and for on-shell pions we obtain

$$F_V(s) = \Gamma_V(s) + T_{11}(s) I_0(s) \Gamma_V(s) \quad (84)$$

The above expression presents a logarithmic divergence which needs one subtraction to be renormalized, choosing the subtraction point s_0 we have a finite form-factor

$$F_V(s) = \Gamma_V(s) + T_{11}(s) (\bar{I}_0(s) + C_V) \Gamma_V(s) \quad (85)$$

$$C_V = -\bar{I}_0(s_0) + \frac{F_V - \Gamma_V}{T_{11} \Gamma_V} \Big|_{s=s_0} \quad (86)$$

Replacing $\bar{I}_0(s) = -T_{11}^{-1}(s) - C_{11} + V_{11}^{-1}(s)$ we get

$$F_V(s) = \frac{T_{11}(s)}{V_{11}(s)} (1 + (C_V - C_{11}) V_{11}(s)) \Gamma_V(s) \quad (87)$$

Notice that Watson’s theorem [36] reads

$$\frac{F_V(s + i\epsilon)}{F_V(s - i\epsilon)} = \frac{T_{11}(s + i\epsilon)}{T_{11}(s - i\epsilon)} = e^{2i\delta_{11}(s)}, \quad s > 4m^2 \quad (88)$$

and it is automatically satisfied. That is a very reassuring aspect of the BSE approach. Indeed, in the literature it is usual [17], [37]– [40] to use Watson’s theorem as an input, and employ it to write a dispersion relation for the form-factor. This procedure leads to so called Omnès–Muskhelishvili [41] representation of the form-factor, which requires the introduction of a polynomial of arbitrary degree. In our case, not only the phase of $F_V(s)$ is fixed, in harmony with Watson’s theorem, but also the modulus, and hence the polynomial, is fixed at the order under consideration.

The normalization of the form factor requires $F_V(0) = 1$, which allows to express the renormalization constant ($C_V - C_{11}$) in terms of T_{11} , Γ_V and V_{11} at $s = 0$, and thus we get

$$F_V(s) = T_{11}(s) \Gamma_V(s) \left\{ \frac{1}{V_{11}(s)} - \frac{1}{V_{11}(0)} + \frac{1}{T_{11}(0)\Gamma_V(0)} \right\} \quad (89)$$

From our formula it is clear that for $s > 4m^2$, where both Γ_V and V_{11} are real, $\text{Re}F(s)^{-1} = 0$ when $\text{Re}T_{11}(s)^{-1} = 0$, in agreement with the vector meson dominance hypothesis. In Eq. (89), T_{11} is obtained from the solution of the BSE for a given “potential”, V_{11} , which admits a chiral expansion, as discussed in Subsect. IV F. The irreducible three-point function, $\Gamma_V(s)$ admits also a chiral expansion of the type

$$\Gamma_V(s) = 1 + \frac{\Gamma_2^V(s)}{f^2} + \dots \quad (90)$$

Note that at lowest order, $\mathcal{O}(p^0)$, $\Gamma_V(0) = F_V(0) = 1$. The next-to-leading function $\Gamma_2^V(s)$ can be obtained if one expands Eq. (89) in powers of $1/f^2$ and compare it to the order $\mathcal{O}(p^2)$ deduced by Gasser-Leutwyler in Ref. [16]. Thus, we get

$$\Gamma_V(s) = 1 + \left\{ \left(1 - \frac{s}{4m^2}\right) \Gamma_2^V(0) + \frac{s}{96\pi^2} \left(\bar{l}_6 - \frac{1}{3}\right) \right\} / f^2 + \dots \quad (91)$$

For $s \gg 4m^2$, $V_{11}(s)$ and $\Gamma_V(s)$ might increase as a power of s , whereas elastic unitarity ensures that $T_{11}(s)$ cannot grow faster than a constant. Indeed, if V_{11} actually diverges or remains at least constant in this limit, then $T_{11}(s)$ behaves like $1/\bar{I}_0(s)$, it is to say, it decreases logarithmically. To guaranty that the elastic form factor goes to zero¹⁶ for $s \rightarrow \infty$, we impose in Eq. (89) the constraint

$$\Gamma_V(0) = V_{11}(0)/T_{11}(0) \quad (92)$$

and thus, we finally obtain

$$F_V(s) = \frac{T_{11}(s) \Gamma_V(s)}{V_{11}(s)} \quad (93)$$

with $\Gamma_V(s)$ given in Eq. (91) and $\Gamma_2^V(0)$ determined by the relation of Eq. (92). Thus, the vector form factor, at this order, is determined by the vector-isovector $\pi\pi$ scattering plus a new low-energy parameter: \bar{l}_6 .

¹⁶This behavior is in agreement with the expected once subtracted dispersion relation for the form factor [13].

2. Scalar form factor

The scalar form factor, $F_S(s)$, is defined by

$$\langle \pi^a(P/2 + k) \pi^b(P/2 - k) | (\bar{u}u + \bar{d}d) | 0 \rangle = \delta^{ab} F_S(s) \quad (94)$$

The scalar form factor is defined through the isospin-zero scalar source, thus the sum over isospin in Eq. (80) selects the $I = 0$ channel. Following the same steps as in the case of the vector form factor we get, after having renormalized,

$$\begin{aligned} F_S(s) &= \frac{T_{00}(s)}{V_{00}(s)} (1 + d_S V_{00}(s)) \Gamma_S(s) \\ d_S &= C_S - C_{00} \end{aligned} \quad (95)$$

where C_S is given by Eq. (86), with the obvious replacements $V \rightarrow S$ and $11 \rightarrow 00$. Watson's theorem is here again automatically satisfied by Eq. (95). A similar discussion as in the case of the vector form-factor leads to set the d_S parameter to zero, since the form factor goes to zero for $s \rightarrow \infty$ [18]. Here again we propose a chiral expansion of the type of Eq. (90) for the irreducible three-point function, $\Gamma_S(s)$

$$\Gamma_S(s) = \Gamma_0^S(s) + \frac{\Gamma_2^S(s)}{f^2} + \dots \quad (96)$$

and expanding the form factor in powers of $1/f^2$ and comparing it to the order $\mathcal{O}(p^2)$ deduced by Gasser-Leutwyler in Ref. [16], we finally get

$$\begin{aligned} \frac{F_S(s)}{F_S(0)} &= \frac{\Gamma_S(s) T_{00}(s) V_{00}(0)}{\Gamma_S(0) T_{00}(0) V_{00}(s)} \\ \frac{\Gamma_S(s)}{\Gamma_S(0)} &= \frac{1}{1 + \frac{1}{f^2} \frac{\Gamma_2^S(0)}{\Gamma_0}} \left\{ 1 + \frac{1}{f^2} \left[\frac{\Gamma_2^S(0)}{\Gamma_0} + \frac{s}{16\pi^2} (\bar{l}_4 + 1 + 16\pi^2 C_{00}) \right] \right\} \\ \frac{\Gamma_2^S(0)}{\Gamma_0} &= - \left(\frac{m^2}{16\pi^2} (\bar{l}_3 + \frac{1}{2}) + \frac{m^2 C_{00}}{2} \right) \\ \Gamma_0^S(s) &= \Gamma_0 = 2B \\ F_S(0) &= 2B \left\{ 1 - \frac{m^2}{16\pi^2 f^2} (\bar{l}_3 - \frac{1}{2}) \right\} \end{aligned} \quad (97)$$

where B is a low energy constant which measures the vacuum expectation value of the scalar densities in the chiral limit [16]. Note that in contrast to the vector case the normalization at zero momentum transfer of the scalar form-factor is unknown.

H. Numerical results: $\pi\pi$ -phase shifts and form-factors.

The lowest order of our approach is obtained by approximating the potential,

$$V_{IJ} \approx \frac{m^2}{f^2} V_{IJ}^{(2)} \quad (98)$$

with $V_{IJ}^{(2)}$ given in Eq. (74). Thus, at this order we have three undetermined parameters C_{00}, C_{11}, C_{20} . At this level of approximation the d -wave phase-shifts are zero, which is not completely unreasonable given their small size, compatible within experimental uncertainties with zero in a region up to 500 MeV. Note that there is a clear parallelism between the C 's parameters here and the $I_0^R(4m^2)$ low energy parameters introduced in Sect. III. Thus, the C 's parameters will be given in terms of the \bar{l}_i parameters, as we found in Subsect. III F, although some constraints on the \bar{l} 's would be imposed since $I_2^R = I_4^R = 0$. However, one should expect more realistic predictions for the phase-shifts in the off-shell case, since there were more freedom to describe the data (four versus three parameters). For the sake of shortness, we do not give here any numerical results for this lowest order of the proposed approximation and also because they do not differ much from those already presented in Subsect. III F. The interesting aspect is that already this lowest order approximation is able to describe successfully the experimental phase shifts for energies above the certified validity domain of ChPT. We come back to this point in Sect. V. In Subsect. IV I we also investigate the convergence of the expansion for the potential, V , proposed in this work. Thus we will compare results at leading (discussed above) and next-to-leading (discussed below) orders for the function W_{IJ} defined in Eq. (66).

Further improvement can be gained by considering the next-to-leading order correction to the potential, which is determined by the approximation:

$$V_{IJ} \approx \frac{m^2}{f^2} V_{IJ}^{(2)} + \frac{m^4}{f^4} V_{IJ}^{(4)} \quad (99)$$

with $V_{IJ}^{(2,4)}$ given in Eq. (74). At next-to-leading, we have nine free parameters (C_{IJ} , with $IJ = 00, 11, 20, 02, 22$ and $\bar{l}_i, i = 1, \dots, 4$) for $\pi\pi$ scattering in all isospin channels and $J \leq 2$. Besides we have two additional ones, (B and \bar{l}_6) to describe the scalar and vector form factors. As we discussed in Eq. (77), in this context the C 's parameters take into account partially the two loop contribution, and thus they could be calculated in terms of the two loop ChPT low energy parameters. That is similar to what we did for the $I_n^R(4m^2)$ parameters in Sect. III or what we could have done above with the C 's parameters at the lowest order of our approach¹⁷. However, we renounce to take to practice this program, because of the great theoretical uncertainties in the determination of the needed two loop ChPT contributions: the two loop contribution have been computed in two different frameworks: ChPT [35] and generalized ChPT [34], and only in the former one a complete quantitative estimate of the low energy parameters is given. Furthermore, this latter study lacks a proper error analysis which has been carried out in Ref. [42]. On top of that a resonance saturation assumption [43] has been relied upon. Therefore, we are led to extract, at least, the C 's parameters from experimental data. For the \bar{l} 's parameters, we could either fit all or some of them to data and fix the remainder to some reasonable values of the literature, as we did

¹⁷In both cases the unknown parameters could be calculated in terms, of the one loop ChPT low energy parameters, \bar{l} 's.

in Subsect. III F. Here, we will follow a hybrid procedure. The justification will be provided *a posteriori*, since the error bars in the \bar{l} 's are reduced in some cases.

1. *Electromagnetic pion form factor.*

Data on $\pi\pi$ scattering are scarce and in most of cases the experimental analysis relies on some theoretical assumptions because of the absence of direct $\pi\pi$ scattering experiments [44]. However, there are direct and accurate measurements on the electromagnetic pion form factor in both the space [45]– and time–like regions [46]. At next-to-leading order, the vector form-factor depends on C_{11} , $\bar{l}_1 - \bar{l}_2$, \bar{l}_4 and \bar{l}_6 (see Eq. (93)). As we did for both sets of parameters in Eq. (29) we take

$$\bar{l}_4 = 4.4 \pm 0.3 \quad (100)$$

as determined by the the scalar radius [18] and fit the another three parameters to the data of Refs. [45] and [46]. Results can be seen both in Fig. 5 and Table II, for different energy cuts.

$\bar{l}_4 = 4.4$	$\sqrt{s} \leq 483$	$\sqrt{s} \leq 700$	$\sqrt{s} \leq 808$	$\sqrt{s} \leq 915$	$\sqrt{s} \leq 1600$
$\bar{l}_1 - \bar{l}_2$	-6_{-2}^{+1}	$-6.1_{-0.3}^{+0.1}$	$-5.92_{-0.04}^{+0.03}$	-5.93 ± 0.03	-5.861 ± 0.010
C_{11}	$-0.15_{-0.05}^{+0.04}$	-0.112 ± 0.010	-0.1099 ± 0.0018	-0.1098 ± 0.0018	$-0.1195_{-0.0015}^{+0.0016}$
\bar{l}_6	19.0 ± 0.3	19.14 ± 0.19	20.84 ± 0.06	20.82 ± 0.06	21.09 ± 0.06
χ^2/dof	1.2	1.2	3.9	3.5	3.3
num. data	63	76	112	126	184

TABLE II. Results of best fits of the next-to-leading approach (Eqs. (65), (93) and (99)) to the electromagnetic pion form factor. Data are taken from Refs. [45] (space–like, $-(503 \text{ MeV})^2 \leq s \leq -(122.47 \text{ MeV})^2$) and [46] (time–like, $320 \text{ MeV} \leq \sqrt{s} \leq 1600 \text{ MeV}$). Errors in the fitted parameters are statistical and have been obtained by increasing the value of χ^2 by one unit. We fix $\bar{l}_4 = 4.4$ and show the variation of the fitted parameters, their statistical errors and χ^2/dof with the used energy cut (given in MeV) for the time–like region. We also give, in the last row the number of piece of data of each of the best fits.

\bar{l}_4	$\bar{l}_1 - \bar{l}_2$	C_{11}	\bar{l}_6
4.1	$-6.2_{-0.3}^{+0.1}$	$-0.112 \pm_{-0.010}^{+0.011}$	19.13 ± 0.19
4.4	$-6.1_{-0.3}^{+0.1}$	-0.112 ± 0.010	19.14 ± 0.19
4.7	$-6.1_{-0.3}^{+0.1}$	-0.111 ± 0.010	$19.15 \pm_{-0.18}^{+0.19}$

TABLE III. Results of best fits of the next-to-leading approach (Eqs. (65), (93) and (99)) to the electromagnetic pion form factor for different values of \bar{l}_4 . Data are taken from Refs. [45] and [46]. In all cases, the fit range is $-503 \text{ MeV} \leq s/|s|^{\frac{1}{2}} \leq 700 \text{ MeV}$. Errors in the fitted parameters are statistical and have been obtained by increasing the value of χ^2 by one unit.

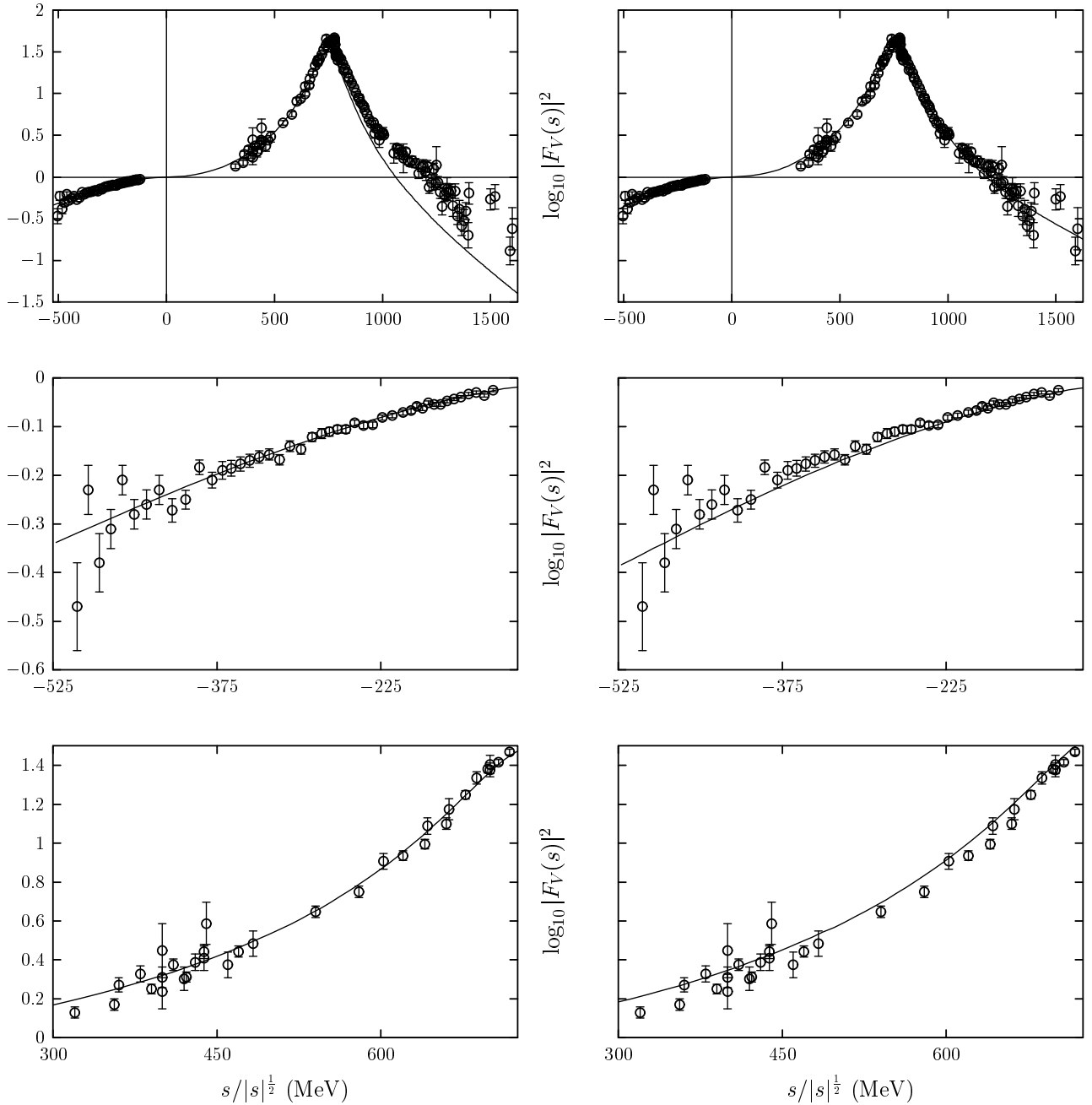


FIG. 5. Best fits of the next-to-leading approach (Eqs. (65) and (93)) to the electromagnetic pion form factor. Data are taken from Refs. [45] (space-like) and [46] (time-like). Results obtained with the parameter set determined by the entry $\sqrt{s} \leq 700$ ($\sqrt{s} \leq 1600$) of Table II are displayed in the left (right) panels.

As can be seen both in the last column of Table II and in the right plots of Fig. 5, a fairly good description of the data from $-500 \text{ MeV} \leq s/|s|^{1/2} \leq 1600 \text{ MeV}$ can be achieved. However, our aim is not only to describe the data but also to determine the low energy parameters which determine the chiral expansion of both the electromagnetic form factor and the $\pi\pi$ -amplitude. If one look at the values of χ^2/dof quoted in Table II, one realizes

that there is a significant change (1.2 versus 3.9) when data above 700 MeV are considered. Besides, the fitted parameters turn out to be not statistically compatible below and above this cut in energies. Although with a small variation on $\bar{l}_1 - \bar{l}_2$, \bar{l}_6 and C_{11} one still gets a reasonable description of the form-factor in the whole range of s , one can appreciate, in the two last rows of plots of Fig. 5, that the higher the energy cut, the worse the description of the low energy region ($-500 \text{ MeV} \leq s/|s|^{\frac{1}{2}} \leq 600 \text{ MeV}$). Indeed, this is the region where the chiral expansion is supposedly more trustable. Neither higher orders in the chiral expansion proposed in this work, nor the effect of non-elastic channels (like 4π and $K\bar{K}$ production) have been included at this level of approximation, and both might account for the discrepancies appreciated in the top left panel of Fig. 5 at high energies. The small changes in the fitted parameters above and below the energy cut of 700 MeV effectively incorporate these new effects into the model. Thus, our best determination of the one-loop ($\bar{l}_1 - \bar{l}_2$ and \bar{l}_6) and two-loop C_{11} low energy parameters come from the best fit with an energy cut of 700 MeV in the time-like region¹⁸. Besides the statistical errors quoted in Table II, we should incorporate some systematics due to the uncertainties in \bar{l}_4 . From the results reported in Table III we deduce that such systematic errors are much smaller than the statistical ones quoted in Table II and can be safely ignored¹⁹. Thus, we get

$$\bar{l}_1 - \bar{l}_2 = -6.1_{-0.3}^{+0.1}, \quad \bar{l}_6 = 19.14 \pm 0.19, \quad C_{11} = -0.112 \pm 0.010 \quad (101)$$

which provides us with an extraordinarily precise determination of the difference $\bar{l}_1 - \bar{l}_2$ and of \bar{l}_6 . The authors of Ref. [18] have completed a two loop calculation for the scalar and vector form factors, finding $\bar{l}_6 = 16.0 \pm 0.5 \pm 0.7$ which differs by as much as two standard deviations from our result.

2. Elastic $\pi\pi$ -scattering in the ρ -channel.

The parameters of Eqs. (100) and (101) uniquely determine, at next-to-leading order in our expansion (Eq. (99)), the vector-isovector $\pi\pi$ scattering phase shifts. Results are shown in Fig. 6. The solid line has been obtained with the central values quoted in Eqs. (100) and (101). There also we show the 68% confidence limits (dashed lines), obtained by assuming uncorrelated Gaussian distributed errors in the parameters quoted in Eqs. (100) and (101) and propagate those to the scattering phase shifts by means of a Monte Carlo simulation. For the difference $\bar{l}_1 - \bar{l}_2$ we have assumed a symmetric error of magnitude 0.3.

¹⁸Lower cuts lead to similar χ^2/dof and statistically compatible fitted parameters, but with appreciably higher errors, as expected from the reduction on the amount of experimental data points. Obviously, we take the highest cut-off, 700 MeV, which keeps the χ^2/dof around one, maximizes the number of data and hence minimizes the errors on the fitted parameters.

¹⁹Vector form factor data are almost insensitive to \bar{l}_4 which has prevented us to determine it from a four parameter fit, but rather to fix it to the value obtained in Ref. [18].

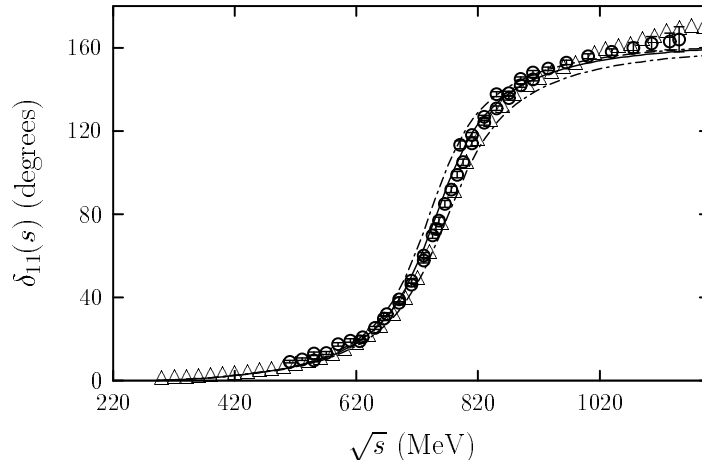


FIG. 6. On-shell next-to-leading order BSE (Eqs. (65) and (99)) vector-isovector phase shifts as a function of the total CM energy \sqrt{s} . The solid line has been obtained using the central values quoted in Eqs. (100) and (101). Dashed lines are the 68% confidence limits assuming Gaussian and uncorrelated error distributions for the parameters. For the difference $\bar{l}_1 - \bar{l}_2$ we have assumed a symmetric error of magnitude 0.3. Circles stand for the experimental analysis of Refs. [21] and [23] and the triangles stand for the Froggatt and Petersen phase-shifts (Ref. [28]) with no errors due to the lack of error estimates in the original analysis.

Besides we also find²⁰

$$m_\rho = 764_{-12}^{+21} \text{ [MeV]}, \quad \Gamma_\rho = 149_{-7}^{+18} \text{ [MeV]} \quad (102)$$

in fairly good agreement with experiment and we also obtain the threshold parameters reported in Table V.

3. Elastic $\pi\pi$ -scattering for s - and d -waves.

In the original work of Gasser-Leutwyler [16] and in the subsequent analysis of Ref. [35] (set **II** in this latter reference) the parameters $\bar{l}_{1,2}$ are measured through the d -wave scattering lengths. Both scattering lengths and specially the isotensor one, suffer from large experimental uncertainties [47] which lead to quite big errors on $\bar{l}_{1,2}$. Here, we have in Eq. (101) a precise determination of the difference $\bar{l}_1 - \bar{l}_2$, thus we can combine it with the experimental measurement of a_{02} to determine both parameters $\bar{l}_{1,2}$. In this way we avoid to use a_{22} , whose relative error is about 13 times bigger than that of a_{02} . We get:

$$\bar{l}_1 = -0.5 \pm 0.5, \quad \bar{l}_2 = 5.6 \pm 0.5 \quad (103)$$

²⁰We use the procedure described in Subsect. III F.

where we have used $m^5 a_{02} = (17 \pm 3) \cdot 10^{-4}$ [47]. The error on the scattering length dominates by far the errors on $\bar{l}_{1,2}$. Fixing \bar{l}_3 from the $SU(3)$ mass formulae [16],

$$\bar{l}_3 = 2.9 \pm 2.4 \quad (104)$$

to complete the analysis of the $\pi\pi$ -scattering at next-to-leading order in our expansion (Eq. (99)), we still have four undetermined parameters (C_{IJ} , with $IJ = 00, 20, 02$, and 22). We determine these four parameters from four independent best fits to the data, fixing the \bar{l}_i parameters to the central values given in Eqs. (100),(103) and (104). Results are reported in Table IV. There, we give C_{IJ} and their statistical errors which have been obtained by increasing the value of the corresponding χ^2 by one unit. In addition to these statistical errors, we have some systematic errors due to uncertainties in the one loop parameters \bar{l}_i . One way of taking into account both types of errors would be to perform a simultaneous eight-parameter (C_{IJ} , with $IJ = 00, 20, 02$, and 22 and $\bar{l}_{1,2,3,4}$) fit to data. However and due to the limited quality of the available experimental data and the multidimensional character of the fit, it is very difficult to single out a stable minimum advising against carrying out this procedure directly. Thus, we have designed an alternative strategy to estimate the systematic uncertainties in the C 's parameters induced by the errors in the one loop parameters. We fix central and statistical errors of the parameters $\bar{l}_{1,2,3,4}$ to the values quoted in Eqs. (100),(103) and (104), and generate a sufficiently large sample of low energy parameters $\bar{l}_{1,2,3,4}$ randomly distributed according to a Gaussian. For each set of four \bar{l} 's parameters we fit, in each angular momentum and isospin channel, the C_{IJ} parameters to the experimental phase shifts. In this way we generate distributions for each of the C 's parameters. For the central values of the C 's parameters we take the results of the fits obtained with the central values of Eqs. (100),(103) and (104)²¹. The 68% confidence limits of each of the distributions give an estimate of the systematic errors in the C 's parameters. Since the out-coming C 's parameter distributions are, in general, not Gaussian we end up with asymmetric errors. Results of this procedure are also reported in Table IV.

A final detail concerns the choice 610 MeV as the energy cut in the scalar-isoscalar channel. This is justified to avoid any possible contamination from the $K\bar{K}$ channel in the sub-threshold region or from higher chiral orders, not included in neither case, at this level of approximation.

Solid lines in Fig. 7 are the predictions for the phase shifts in each angular momentum-isospin channel. At each fixed CM energy, our prediction for the phase shift will suffer from uncertainties due to both the statistical errors on \bar{l}_i and C_{IJ} parameters and also the systematic errors on the latter ones induced by the statistical fluctuations of the former ones,

²¹This is not the same as computing the mean of the generated distribution. Indeed, the mean values in general can not be obtained from any specific choice of the input parameters, in this case the \bar{l} 's. This is the reason to quote central values from results obtained from central values of the input parameters. Furthermore, the statistical errors obtained before by changing the χ^2 by one unit, are referred to the values resulting from best fits to the data with input parameters fixed to their central values. Both choices do not differ much as long as we are dealing with relatively small asymmetries in the distributions. We should stress that, what it is statistically significant is the 68% error band rather than the choice of the central value.

as we discussed above. We use a Monte Carlo simulation to propagate independently both sources of errors and finally we add in quadratures, respecting the possible asymmetries, the statistical and systematic phase shift errors. The dashed lines in Fig. 7 join the central value for the phase-shift plus its upper total error or minus its lower total error for every CM energy. We see that, in general, the agreement with experiment is good except for the scalar–isoscalar channel, where one clearly sees that there is room for contributions due to the $K\bar{K}$ inelastic channel above the energy cut (610 MeV) used for the best fit.

IJ	00	20	02	22
C_{IJ}	$-0.022^{+0.001+0.005}_{-0.001-0.003}$	$-0.058 \pm 0.002^{+0.025}_{-0.002}$	$-0.203 \pm 0.003^{+0.080}_{-0.300}$	$-0.5 \pm 0.2^{+0.5}_{-0.3}$
$\chi^2/\text{num. data}$	34.7 / 20	20.5 / 21	11.4 / 24	0.4 / 24

TABLE IV. Next-to-leading (Eq. (99)) parameters fitted to the experimental data of Refs. [21] – [26] (with an energy cut of 610 MeV) for $I = J = 0$, of Refs. [27] and [48] for $I = 2$, $J = 0$ and finally of Ref. [23] (with an energy cut of 970 MeV) for the d -wave channels. In the latter case and due to the lack of error estimates in the original references, we have assumed an error of 0.4 in all phase shifts, this assumes that the errors of the d -wave phase-shifts given in Ref. [23], affect only to the last digit. The central values and statistical errors of the parameters $\bar{l}_{1,2,3,4}$ have been fixed to the values quoted in Eqs. (100),(103) and (104). We give two sets of errors in the fitted parameters. The first set corresponds to statistical errors and have been obtained by increasing the value of the corresponding χ^2 by one unit. The second set are systematic, induced by the uncertainties in $\bar{l}_{1,2,3,4}$, and have been estimated by means of a Monte Carlo simulation, see text for details.

IJ	00	11	20	02	22
$m^{2J+1}a_{IJ}$	$0.216^{+0.004}_{-0.006}$	0.0361 ± 0.0003	-0.0418 ± 0.0013	input	0.00028 ± 0.00012
(exp)	0.26 ± 0.05	0.038 ± 0.002	-0.028 ± 0.012	0.0017 ± 0.0003	0.00013 ± 0.00030
$m^{2J+3}b_{IJ}$	$0.284^{+0.009}_{-0.014}$	0.0063 ± 0.0005	$-0.075^{+0.002}_{-0.003}$	$-\frac{481}{201600} \frac{m^4}{\pi^3 f^4}$	$-\frac{277}{201600} \frac{m^4}{\pi^3 f^4}$
(exp)	0.25 ± 0.03		-0.082 ± 0.008		

TABLE V. Threshold parameters a_{IJ} and b_{IJ} (obtained from an expansion of the scattering amplitude [29], $\text{Re}T_{IJ} = -16\pi m(s/4 - m^2)^J [a_{IJ} + b_{IJ}(s/4 - m^2) + \dots]$ close to threshold) deduced from the $\mathcal{O}(p^4)$ results reported in Table. IV and Eq. (101). For all channels, except for the $I = J = 1$ one, the errors have been obtained by adding in quadratures those induced by the uncertainties in the \bar{l} 's parameters and those induced by the experimental errors in the $\pi\pi$ phase-shifts. For the vector-isovector channel, the error treatment is simpler thanks to the simultaneous determination of $\bar{l}_1 - \bar{l}_2$ and C_{11} from a best fit to data and to the negligible effect of the error bars of \bar{l}_4 on the latter fit. Thus in this channel, uncertainties have been obtained by assuming uncorrelated Gaussian distributed errors in the parameters quoted in Eqs. (100) and (101). We also give the known experimental values compiled in Ref. [49].

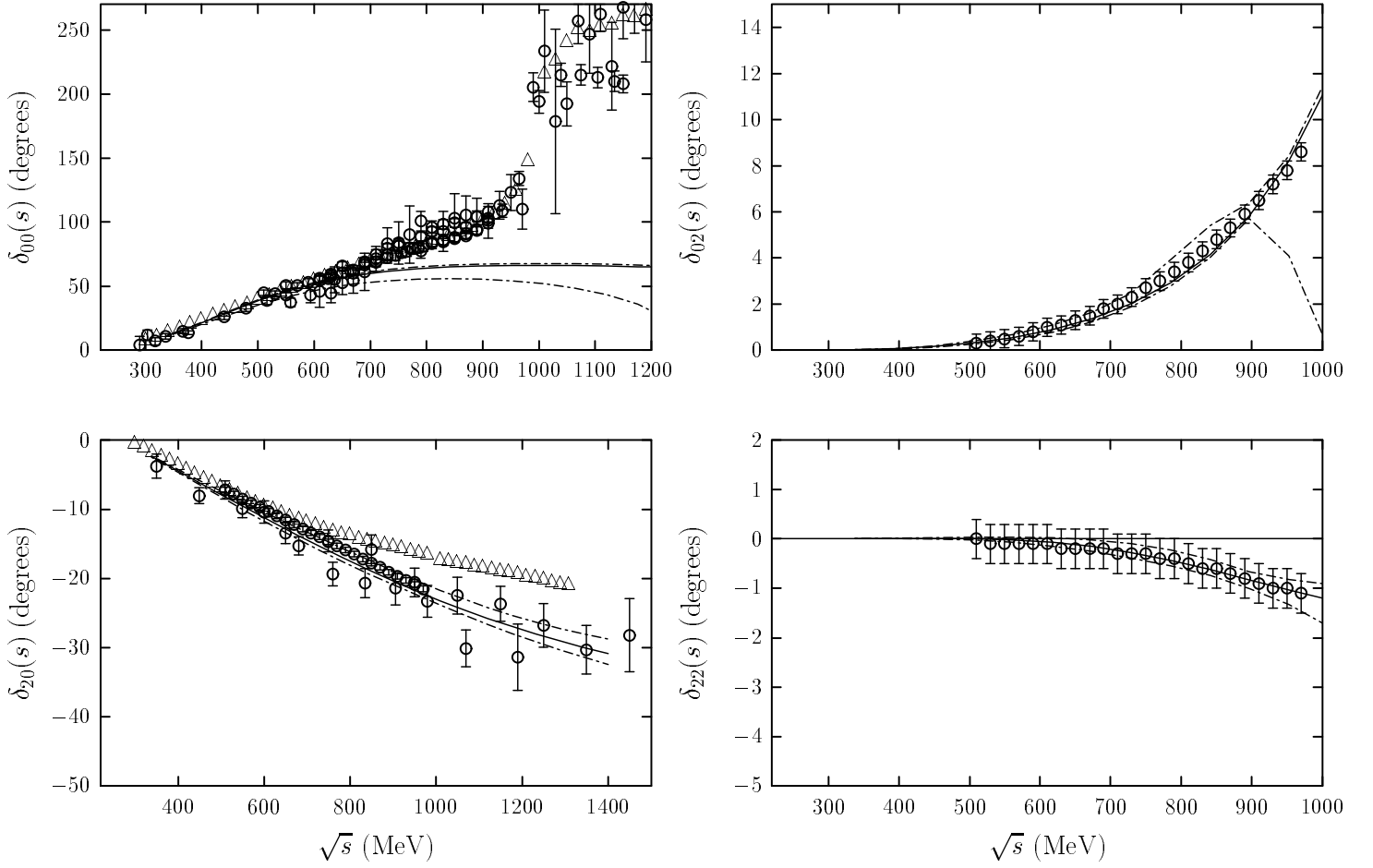


FIG. 7. Several $\pi\pi$ phase shifts as a function of the total CM energy \sqrt{s} obtained within our next-to-leading approximation (see Eq. (99)). The top (bottom) panels correspond to $I = 0$ (2) whereas the left (right) panels correspond to $J = 0$ (2). Experimental data are taken from Refs. [21] – [26] ($I = J = 0$) from Refs. [27] and [48] ($I = 2, J = 0$) and finally from Ref. [23] for the d -wave channels. Triangles stand for the Froggatt and Petersen phase-shifts (Ref. [28]) with no errors due to the lack of error estimates in the original analysis. Solid lines have been obtained with the central values quoted in Table IV and in Eqs. (100),(103) and (104). Dashed lines show our total uncertainties, statistical and systematic, added in quadratures, see text for more details.

In Table V we also give the deduced threshold parameters. We propagate both types of errors discussed above to these observables, by means of a Monte Carlo simulation, and finally we add both errors in quadratures. In general, for those parameters which have been measured, we find agreement within experimental uncertainties, though our final errors are always significantly smaller than the experimental ones compiled in Ref. [49].

4. Numerical comparison with two loop ChPT.

	Set	(tree)	+(1loop)	+(2loop)	total	experiment
a_{00}	I		0.044 ± 0.005	0.016 ± 0.003	0.216 ± 0.009	0.26 ± 0.05
	II	0.156	0.039 ± 0.008	0.013 ± 0.003	0.208 ± 0.011	
	BSE		0.045 ± 0.004	$0.011^{+0.001}_{-0.002}$	$0.216^{+0.004}_{-0.006}$	
b_{00}	I		0.069 ± 0.010	0.027 ± 0.007	0.275 ± 0.016	0.25 ± 0.03
	II	0.179	0.059 ± 0.024	0.019 ± 0.011	0.256 ± 0.034	
	BSE		0.072 ± 0.009	$0.006^{+0.005}_{-0.009}$	$0.284^{+0.009}_{-0.014}$	
$10 \cdot a_{11}$	I		0.073 ± 0.010	0.025 ± 0.006	0.395 ± 0.014	0.38 ± 0.02
	II	0.297	0.058 ± 0.033	0.018 ± 0.005	0.374 ± 0.034	
	BSE		0.064 ± 0.003	0	0.361 ± 0.003	
$10 \cdot b_{11}$	I		0.048 ± 0.006	$0.031^{+0.005}_{-0.007}$	$0.080^{+0.007}_{-0.009}$	—
	II	0	0.034 ± 0.033	$0.020^{+0.005}_{-0.008}$	0.054 ± 0.029	
	BSE		0.0389 ± 0.0017	0.021 ± 0.003	0.063 ± 0.005	
$10 \cdot a_{20}$	I		0.028 ± 0.018	0.004 ± 0.002	-0.414 ± 0.020	-0.28 ± 0.12
	II	-0.446	0.008 ± 0.031	$0.000^{+0.002}_{-0.003}$	-0.438 ± 0.032	
	BSE		0.028 ± 0.016	$0.000^{+0.003}_{-0.004}$	-0.418 ± 0.013	
$10 \cdot b_{20}$	I		0.17 ± 0.04	0.01 ± 0.01	-0.72 ± 0.04	-0.82 ± 0.08
	II	-0.89	0.10 ± 0.05	0.00 ± 0.01	-0.79 ± 0.05	
	BSE		0.16 ± 0.04	$0.01^{+0.01}_{-0.02}$	$-0.75^{+0.02}_{-0.03}$	
$10^2 \cdot a_{02}$	I		0.181 ± 0.025	0.079 ± 0.016	0.260 ± 0.036	0.17 ± 0.03
	II	0	0.117 ± 0.026	0.053 ± 0.018	0.170 ± 0.030	
	BSE		0.170 ± 0.030	0	input	
$10^3 \cdot a_{22}$	I		0.21 ± 0.13	$-0.01^{+0.06}_{-0.04}$	0.20 ± 0.10	0.13 ± 0.30
	II	0	0.12 ± 0.44	$0.01^{+0.17}_{-0.12}$	0.13 ± 0.30	
	BSE		0.28 ± 0.12	0	0.28 ± 0.12	

TABLE VI. Separation in powers of $1/f^2$ of some of the threshold parameters reported in Table V. For comparison we have also compiled the results reported in Table 1 of Ref. [42] which are obtained from the two-loop analysis of Ref. [35] supplemented with proper error estimates. The Sets **I** and **II** refer to those define in Ref. [35]. The authors of Ref. [35] assume some resonance saturation to give numerical values to the $\mathcal{O}(p^6)$ parameters at certain scale around 750 MeV (see that reference for details). In addition, Set **I** uses: $\bar{l}_1 = -1.7 \pm 1.0, \bar{l}_2 = 6.1 \pm 0.5, \bar{l}_3 = 2.9 \pm 2.4, \bar{l}_4 = 4.3 \pm 0.9$ and Set **II** uses: $\bar{l}_1 = -0.8 \pm 4.8, \bar{l}_2 = 4.45 \pm 1.1, \bar{l}_3 = 2.9 \pm 2.4, \bar{l}_4 = 4.3 \pm 0.9$. On the other hand, BSE stands for the results of the present work at next-to-leading order, with parameters given in Table IV and Eqs. (100), (101), (103), and (104). Tree, one-loop, two-loops and total labels stand for the threshold parameters calculated at $\mathcal{O}(p^2)$, $\mathcal{O}(p^4)$, $\mathcal{O}(p^6)$ and all orders, respectively. We also give the known experimental values compiled in Ref. [49]. All threshold parameters are given in pion mass units. Note, that due to correlations between the several orders, in the $1/f^2$ expansion, contributing to the threshold observables, the errors of the total quantities can not be simply added in quadratures; we use a Monte Carlo simulation to propagate errors.

A very interesting feature of the present treatment at next-to-leading order is that having fitted the C 's to the data, we can use those parameters to learn about the two and even higher loop contributions (see Eq. (77)). The separation of the amplitudes near threshold, in powers of $1/f^2$, is presented in Table VI, and compared to recent two loop ChPT calculations [35] supplemented with proper error estimates [42]. Despite of the resonance saturation hypothesis²² assumed in Refs. [35,42], in general we see that the BSE predictions are not less accurate than those of these references. Both sets of results, BSE and ChPT, suffer from systematic errors induced by the higher order contributions. Those are not included in either case.

5. Scalar pion form factor.

To end this subsection, in Fig. 8, we present results for the scalar form-factor (Eq. (97)), normalized to one at $s = 0$ and computed at next-to-leading order accuracy, within our approach. It is to say, it uses, $V_{00}(s)$ given in Eq. (99) with the parameters presented in Eqs. (100),(103) and (104) and Table IV. We also compare our results with those obtained in Ref. [40]. Our results disagree with those of Ref. [40] above 500 MeV, presumably due to the role played by the sub-threshold $K\bar{K}$ effects.

I. Comparison of leading and next-to-leading on-shell BSE predictions.

In this subsection we compare results for elastic $\pi\pi$ -scattering at leading and next-to-leading accuracy within the on-shell BSE scheme. This kind of comparison is not generally undertaken in the literature regarding unitarization methods, where the main goal is just to fit the data, rather than study also the convergence of the expansion. Since in our framework, the potential plays the central role, such a comparison is naturally done in terms of it or in terms of the function $W_{IJ}(s) = T_{IJ}^{-1}(s) + \bar{I}_0(s)$ defined in Eq. (66). These W_{IJ} functions can be directly extracted from data²³, in other words, they can be derived from experimental phase-shifts. In Fig. 9 we present experimental, BSE-leading and -next-to-leading results²⁴, together with both experimental and theoretical error estimates, for $W_{00}^{-1}, W_{20}^{-1}, W_{02}, W_{22}$

²²Such an approximation reduces a priori the errors on the two loop contributions with respect to the present framework where these higher order corrections have to be fitted directly to experimental data.

²³Note, the functions V_{IJ} can not directly be obtained from experiment, because of the unknown constants C_{IJ} .

²⁴Note, that because the presence of resonances in the σ - and ρ -channels, the corresponding W -functions should have a pole (see discussion related to Fig. 3), so we present the inverse for these channels and also, for a better comparison, for the isotensor-scalar one. On the other hand for d - waves the lowest BSE order approximation gives $T = 0$, and therefore for those channels we present W itself.

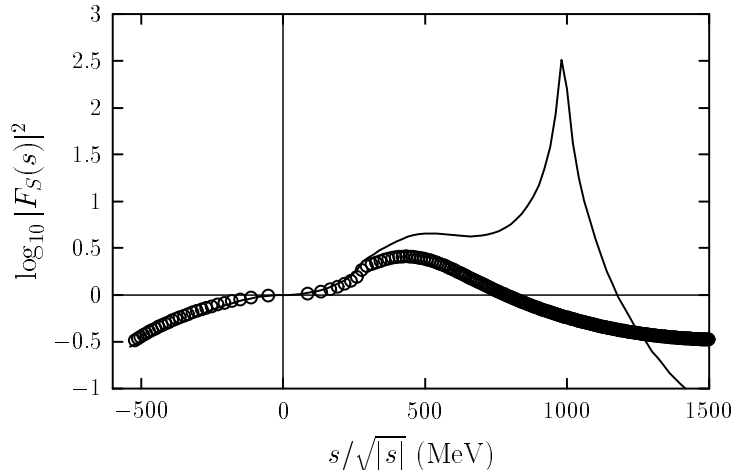


FIG. 8. On-shell next-to-leading order BSE (Eqs. (97) and (99)) scalar form factor (circles) as a function of s . The used parameters are those given in Eqs. (100),(103) and (104) and Table IV. For comparison we also show the results of Refs. [40] (solid line).

and W_{11}^{-1} . Next-to-leading results are obtained from Eq. (99). Central values and uncertainties of the needed low energy constants were discussed in Subsect. IV H (Table IV and Eqs. (100), (101), (103), and (104)). Errors have been propagated via a MonteCarlo simulation and statistical and systematic errors have been added in quadratures. Leading results have been obtained from Eq. (98) where the unknown low energy constants C_{00} , C_{11} and C_{20} have been obtained from three one parameter best fits to the experimental data, since at lowest order the three channels are independent. For the s -wave channels we have fitted the same set of data and use the same energy cuts as in Table IV and Fig. 7. We have obtained

$$C_{00} = -0.0273 \pm 0.0004 \quad \chi^2/\text{num. data} = 31.2/20 \quad (105)$$

$$C_{20} = -0.051 \pm 0.014 \quad \chi^2/\text{num. data} = 21.4/21$$

For these two channels both leading and next-to-leading approximations provide similar descriptions of the data. For the ρ -channel the situation is different. We have fitted C_{11} to the data of Ref. [21]. Fits from threshold up to 0.9 GeV give values of χ^2/dof of the order of 12, being then highly unlikely that such a big discrepancy between theory and data is due to statistical fluctuations, disqualifying any error analysis. We find significantly lower values of χ^2/dof for smaller energy cuts, being the optimum choice obtained with a energy cut of about 690 MeV, for which we find:

$$C_{11} = -0.1275 \pm 0.0006 \quad \chi^2/dof = 4.1 \quad (106)$$

The above error is quite small, due to large value of χ^2 . Leading and next-to-leading estimates for all three parameters C_{00} , C_{20} and C_{11} are compatible within two sigmas.

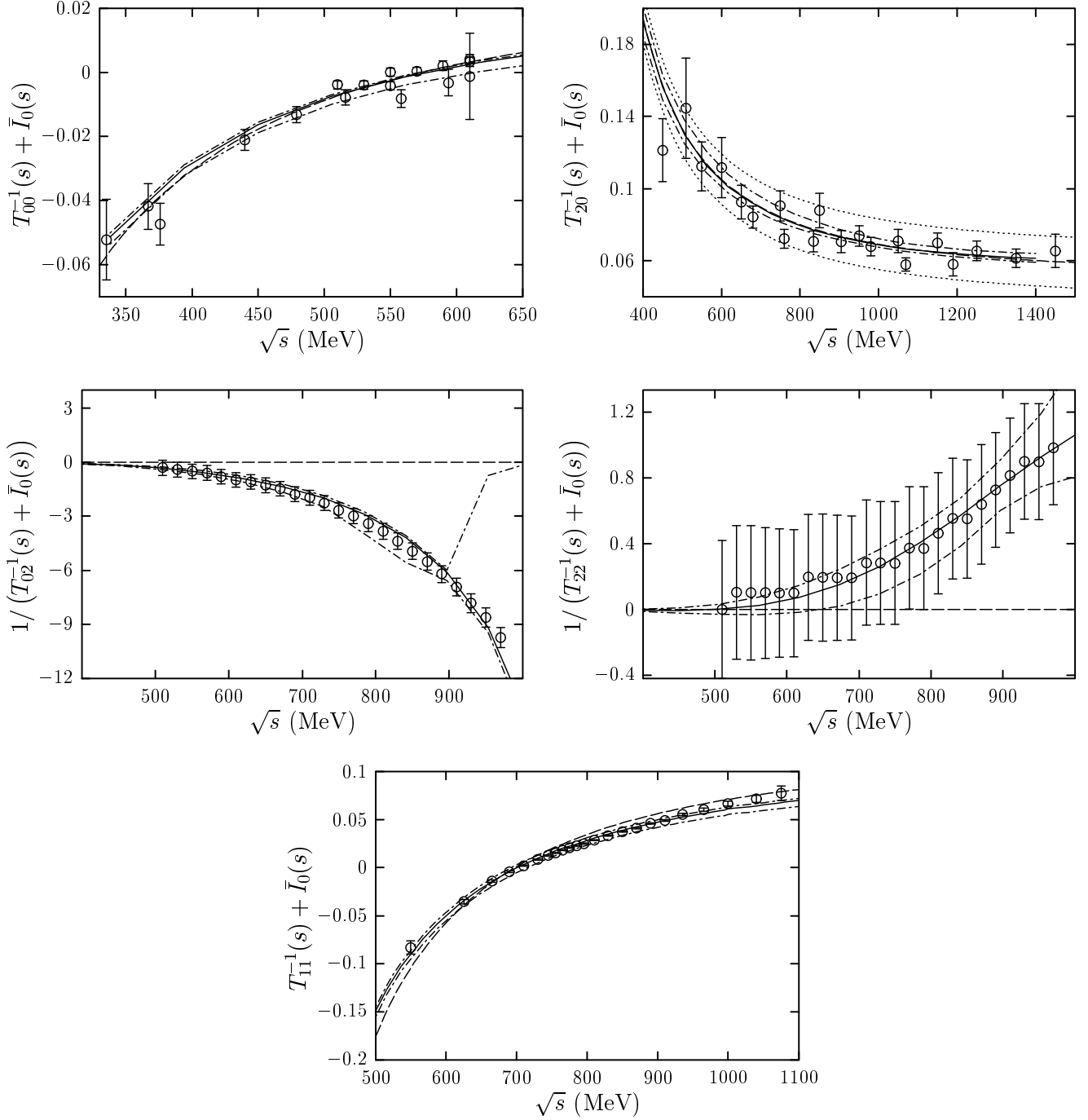


FIG. 9. Experimental (circles), BSE-leading (dashed lines) and -next-to-leading (solid lines) results, together with both experimental and theoretical (dash-dotted and dotted lines for leading and next-to-leading predictions respectively) error estimates, for W_{00}^{-1} , W_{20}^{-1} , W_{02} , W_{22} and W_{11}^{-1} as a function of the CM energy. In some cases the theoretical errors can not be seen due to their smallness. See Subsect. IV I for more details.

Results from Fig. 9 show a good rate of convergence of the expansion proposed in this work.

V. THE NON-PERTURBATIVE NATURE OF THE C_{IJ} PARAMETERS.

In this section we link the renormalization C_{IJ} parameters to some non-perturbative effects of the underlying theory, such as the the existence of resonances.

For simplicity, let us consider the ρ -channel ($I = J = 1$) for which the lowest order inverse amplitude, within the on-shell scheme (Eq. (98)), reads

$$T_{11}^{-1}(s) - T_{11}^{-1}(-\mu^2) = -\left(\bar{I}_0(s) - \bar{I}_0(-\mu^2)\right) - 6f^2 \left(\frac{1}{s - 4m^2} + \frac{1}{\mu^2 + 4m^2}\right) \quad (107)$$

where we have chosen the subtraction point $s_0 = -\mu^2$. From above, we identify C_{11} by

$$C_{11} = -T_{11}^{-1}(-\mu^2) - \bar{I}_0(-\mu^2) + \frac{6f^2}{\mu^2 + 4m^2} \quad (108)$$

which should be independent of the scale μ^2 . Thus we have

$$T_{11}^{-1}(s) = -\left(\bar{I}_0(s) + C_{11}\right) - \frac{6f^2}{s - 4m^2} \quad (109)$$

At the resonance, $s = m_\rho^2$, $\text{Re } T_{11}(m_\rho^2)^{-1} = 0$, and thus if we look at the real parts, we have

$$\begin{aligned} C_{11} &= -\text{Re } \bar{I}_0(m_\rho^2) - \frac{6f^2}{m_\rho^2 - 4m^2} \\ &= -\frac{1}{16\pi^2} \log \frac{m_\rho^2}{m^2} - \frac{6f^2}{m_\rho^2} + \mathcal{O}\left(\frac{m^2}{m_\rho^2}\right) \\ &\approx -0.110 \end{aligned} \quad (110)$$

in qualitative good agreement with the findings of previous sections (see, for instance, the I_0^R entries for this channel in Table I or Eq. (101)).

Similarly for the scalar-isoscalar channel,

$$T_{00}^{-1}(s) - T_{00}^{-1}(-\mu^2) = -\left(\bar{I}_0(s) - \bar{I}_0(-\mu^2)\right) - f^2 \left(\frac{1}{s - m^2/2} + \frac{1}{\mu^2 + m^2/2}\right) \quad (111)$$

where we have chosen the subtraction point $s_0 = -\mu^2$ and it can be different for each IJ channel since we may take $T_{IJ}(-\mu^2)$ as the fitting and *a priori* unknown parameter. As before, we can identify C_{00}

$$C_{00} = -T_{00}^{-1}(-\mu^2) - \bar{I}_0(-\mu^2) + \frac{f^2}{\mu^2 + m^2/2} \quad (112)$$

From all our previous discussions and fits it is rather clear that in the $I = J = 0$ channel the σ resonance cannot be completely understood without inclusion of sub-threshold $K\bar{K}$ contributions. Nevertheless, let us define the point $s = m_\sigma$ as the one fulfilling $\text{Re } T_{00}(m_\sigma^2)^{-1} = 0$, yielding

$$\begin{aligned}
C_{00} &= -\text{Re} \bar{I}_0(m_\sigma^2) - \frac{f^2}{m_\sigma^2 - m^2/2} \\
&= -\frac{1}{16\pi^2} \log \frac{m_\sigma^2}{m^2} - \frac{f^2}{m_\sigma^2} + \mathcal{O}\left(\frac{m^2}{m_\sigma^2}\right) \\
&\approx -0.043
\end{aligned} \tag{113}$$

for $m_\sigma = 600$ MeV. This is not completely unreasonable since the phase shift at about $s = 600\text{MeV}$ go up to 60° , which is equivalent to take $\text{Re} T_{00}(m_\sigma^2)^{-1}$ small. From this discussion, we understand the origin of the significant difference of size between C_{11} and C_{00} . Indeed, neglecting the logarithmic contributions,

$$\frac{C_{11}}{C_{00}} \approx 6 \frac{m_\sigma^2}{m_\rho^2} \tag{114}$$

which clearly points out that the reason for the different size between the two C parameters relies on the fact that the potential in the ρ -channel is about six times smaller than that in the scalar-isoscalar one. This has also been pointed out by the authors of Ref. [50] who also use this argument to stress the dominant role played by unitarization in the σ channel. The authors of this same work, also claim that the quite different values of C_{00} and C_{11} could not be understood if the same scale or cutoff, as they used in a previous work [9], are used for both channels. Indeed, if one uses dimensional regularization to compute the divergent integral $I_0(s)$ and in the $\overline{\text{MS}}$ scheme, one gets the finite piece

$$I_0^D(s) = \frac{1}{16\pi^2} \left\{ -2 + \log \frac{m^2}{\nu^2} \right\} + \bar{I}_0(s) \tag{115}$$

being ν some renormalization scale. Thus, one might identify

$$C = \frac{1}{16\pi^2} \left\{ -2 + \log \frac{m^2}{\nu^2} \right\} \tag{116}$$

for all angular momentum and isospin channels. The above equation gives values for the C parameter of about -0.04 when scales, ν , of the order 1 GeV are used. This agrees reasonably well with the values found for C_{00} , but to get values of about -0.11 , as it is the case for C_{11} , one needs unrealistic scales or cut-offs of the order of 300 GeV. All confusion, comes from the interpretation of the C parameter as a renormalization of the bubble divergent integral $I_0(s)$, instead of a renormalization of the full amplitude once that a renormalized potential is iterated by means of the BSE. A direct, comparison of Eqs. (116) and (108) or (112) shows that the *free* parameters $T_{IJ}(-\mu^2)$ allow for the use of the same value of the scale μ to generate such different values for the C_{IJ} parameters in the scalar-isoscalar and vector-isovector channels. Furthermore, as we said above, the C parameters defined in Eq. (108) or (112) do not depend on scale. On the light of this discussion, the numerical coincidence between the values provided by Eq. (116) and C_{00} might be considered accidental.

From the former expressions and neglecting corrections of the order of the $\mathcal{O}(m^2/m_{\rho,\sigma}^2)$ we find simple expressions for the amplitudes in the two channels considered in this section,

$$\begin{aligned}
T_{11}^{-1}(s) &\approx -\frac{1}{16\pi^2} \log\left(-\frac{s}{m_\rho^2}\right) - 6f^2\left(\frac{1}{s} - \frac{1}{m_\rho^2}\right) \\
T_{00}^{-1}(s) &\approx -\frac{1}{16\pi^2} \log\left(-\frac{s}{m_\sigma^2}\right) - f^2\left(\frac{1}{s} - \frac{1}{m_\sigma^2}\right)
\end{aligned} \tag{117}$$

where we take $\log(-s/m_R^2) = \log(|s|/m_R^2) - i\pi\Theta(s)$. The above expressions lead to approximate expressions for the decay widths (see Eq. (30))

$$\Gamma_\rho = \frac{m_\rho^3}{96\pi f^2} \frac{1}{1 - \frac{m_\rho^2}{96\pi^2 f^2}} \quad (118)$$

$$\Gamma_\sigma = \frac{m_\sigma^3}{16\pi^2 f^2} \frac{1}{1 - \frac{m_\sigma^2}{16\pi^2 f^2}} \quad (119)$$

For the ρ -channel, this corresponds to a coupling $g_{\rho\pi\pi} \approx (m_\rho/\sqrt{2}f)$, the value predicted by the KSFR relation [51]. KSFR predicts, for $m_\rho = 770$ MeV a width of $\Gamma_\rho = 141$ MeV, in excellent agreement with the experimental value. Such a derivation of the KSFR relation is actually not completely unexpected since this relation is a consequence of PCAC plus vector meson dominance through current-field identities; in our model vector meson dominance is realized, i.e. the real parts of the inverse scattering amplitude in the $I = J = 1$ channel and of the inverse vector form factor vanish simultaneously, as we pointed out after Eq. (89). The width for the σ meson turns out to be very large making this way of determining it doubtful. Notice that in both cases the conditions for non negative widths are $m_\rho^2 < 96\pi^2 f^2$ and $m_\sigma^2 < 16\pi^2 f^2$ respectively.

VI. COMPARISON WITH OTHER UNITARY APPROACHES

As we have hopefully pointed out along this work, the unitarization generated through a solution of the BSE becomes extremely important to describe the resonance region and also “guides” the theory in the low energy regime, allowing for a reasonably accurate description of low energy and threshold parameters.

In what follows we want to compare the BSE with some other approaches pursued in the literature for on-shell amplitudes which also incorporate elastic unitarity. Some of the methods presented here have already been discussed, [52], in the chiral limit.

All unitarization schemes provide the same imaginary part for the inverse amplitude and they differ in the way the real part is approximated. Thus, it is not surprising that formal relations among them can be found.

A. K-matrix

A usual unitarization method consists in working with the K -matrix, defined as

$$K_{IJ}^{-1} = \text{Re}(T_{IJ}^{-1}) = T_{IJ}^{-1} - i\rho$$

$$\rho = -\text{Im}\bar{I}_0(s + i\epsilon) = \frac{\lambda^{\frac{1}{2}}(s, m^2, m^2)}{16\pi s} = \frac{1}{16\pi} \sqrt{1 - \frac{4m^2}{s}} \quad (120)$$

In the bottom graph of Fig. 3, we plot the inverse of the K -matrix for the isovector p -wave channel. The presence of a pole (zero in the inverse function) in K_{11} limits the use of any “perturbative” expansion of K_{11} in the region of the resonances and this fact prevents the use of this unitarization scheme above threshold when there exists a resonance.

B. Dispersive Representation of the Inverse of the Partial Wave Amplitude.

Partial wave amplitudes, T_{IJ} , have both right and left hand cuts. Besides, the only poles that are allowed on the physical s sheet are the bound states poles, which occur on the positive real axis below $4m^2$. Poles on the real axis above threshold violate unitarity, and those on the physical sheet that are off the real axis violate the Mandelstam hypothesis [32] of maximum analyticity. Thus, T_{IJ} and T_{IJ}^{-1} have similar right and left cuts. However, partial wave amplitudes have zeros, which in turn means that their inverses have poles on the physical sheets.

A seemingly significant advantage of considering the dispersive representation of the inverse of a partial wave amplitude is that its right hand cut discontinuity is just given by phase space in the elastic region, thanks to unitarity. The relevance of this property was already emphasized in Ref. [6]. For simplicity, let us suppose that T_{IJ} , has a zero of order 1 for $s = s_A$ ²⁵.

If we define,

$$r = \lim_{s \rightarrow s_A} (s - s_A) T_{IJ}^{-1}(s) \quad (121)$$

assuming that $|T_{IJ}^{-1}(s)| < s$ as $s \rightarrow \infty$ then each inverse amplitude satisfies a once-subtracted dispersion relation [6], with $s = s_1$, the subtraction point (dropping the labels I, J for simplicity)

$$\begin{aligned} T^{-1}(s) - T^{-1}(s_1) &= \left(\frac{r}{(s - s_A)} - \frac{r}{(s_1 - s_A)} \right) + \frac{(s - s_1)}{\pi} \int_{4m^2}^{\infty} \frac{ds'}{(s' - s_1)(s' - s)} \text{Im} T^{-1}(s') \\ &+ \frac{(s - s_1)}{\pi} \int_{-\infty}^0 \frac{ds'}{(s' - s_1)(s' - s)} \text{Im} T^{-1}(s') \end{aligned} \quad (122)$$

Elastic unitarity (Eq. (26)) allows to perform the integral over the right hand cut, thus one gets

$$\begin{aligned} T^{-1}(s) - T^{-1}(s_1) &= \left(\frac{r}{(s - s_A)} - \frac{r}{(s_1 - s_A)} \right) - (\bar{I}_0(s) - \bar{I}_0(s_1)) \\ &+ \frac{(s - s_1)}{\pi} \int_{-\infty}^0 \frac{ds'}{(s' - s_1)(s' - s)} \text{Im} T^{-1}(s') \end{aligned} \quad (123)$$

Then one clearly sees that all the dynamics of the process is contained in both the poles of T^{-1} (zeros of T) and in the left hand cut. This latter contribution can be split as follows:

$$\frac{(s - s_1)}{\pi} \int_{-\infty}^0 \frac{ds'}{(s' - s_1)(s' - s)} \text{Im} T^{-1}(s') = \frac{1}{\mathcal{V}(s)} - \frac{1}{\mathcal{V}(s_1)} \quad (124)$$

²⁵For the s -waves, these are demanded by the Adler condition, for the p -waves, the zero is kinematic being at threshold, $s_A = 4m^2$. In both latter cases, the zeros are of order one, higher partial waves have higher order zeros.

where

$$\frac{1}{\mathcal{V}(s)} = \frac{1}{\pi} \int_{-\infty}^0 \frac{ds'}{(s' - s)} \text{Im}T^{-1}(s') + P \quad (125)$$

where P is a renormalization constant, though in general might be a polynomial. Thus, $T^{-1}(s)$ can be written as

$$T^{-1}(s) = -\bar{I}_0(s) - k + \frac{r}{s - s_A} + \mathcal{V}^{-1}(s) \quad (126)$$

being k a constant. The above equation with the obvious replacements is identical to Eq. (65). As a final remark to this method, we add that the solution to the dispersion relation is not unique (any pair of solutions with different values of the constant k satisfy the same dispersion relation), since we may include any zeros to the inverse amplitude, which become poles in the amplitude. In the particular case of $\pi\pi$ scattering such poles are inadmissible, so an additional condition on the constant k has to be imposed to describe the physics.

C. Blackenbekler Sugar type equations

It is interesting to see that many of our considerations are strongly related to a Blackenbekler-Sugar type equation [53]. Let us consider the BSE in operator form,

$$T = V + VG_0T \quad (127)$$

As we know the “potential” V is the two particle irreducible amputated Green function. Thus, it does not contribute to the s -channel unitarity cut, i.e. $\text{Disc}[V_{pk}(s)] = 0$ for $s > 4m^2$. On the other hand, the s -channel two particle reducible diagrams do contribute to the unitarity cut, but the part of them which does not contribute to the discontinuity is not uniquely defined. The idea is to split the two particle propagator into two parts, one containing the elastic unitarity cut and the rest. This separation is ambiguous, since we can sum to the former any function with no discontinuity. A practical way to do this is as follows. We write

$$G_q(s) = \Delta(q_+)\Delta(q_-) = \bar{G}_q(s) + g_q(s) \quad (128)$$

where we impose that

$$\text{Disc}[G_q(s)] = \text{Disc}[\bar{G}_q(s)] = (-2\pi i)\delta^+[q_+^2 - m^2](-2\pi i)\delta^+[q_-^2 - m^2], \quad s > 4m^2 \quad (129)$$

A solution to this discontinuity equation is²⁶

$$\bar{G}_q(s) = -i\pi \frac{\delta(P \cdot q)}{q^2 - m^2 + s/4 + i\epsilon} \quad (130)$$

²⁶ Notice the identity $(-2\pi i)^2\delta^+[q_+^2 - m^2]\delta^+[q_-^2 - m^2] = -2\pi^2\delta(P \cdot q)\delta(q^2 - m^2 + \frac{s}{4})$

This, of course, is not the only choice; we could equally well add a polynomial to $\bar{G}_q(s)$ without changing the discontinuity. Proceeding in perturbation theory we can see that

$$T = V + V(\bar{G}_0 + g)T = t + t\bar{G}_0T \quad (131)$$

where $t = V + Vgt = V + VgV + VgVgV + \dots$

Thus we are finally led to a equation of the form

$$T_P(p, k) = t_P(p, k) + \pi \int \frac{d^4q}{(2\pi)^4} T_P(q, k) \frac{\delta(P \cdot q)}{q^2 - m^2 + \frac{s}{4} + i\epsilon} t_P(p, q) \quad (132)$$

This equation looks like the Blackenbecker-Sugar equation [53] but with the important difference that instead of the potential $V_P(p, k)$ we iterate the reduced amplitude $t_P(p, k)$ which at lowest order in $1/f^2$ coincides with the original potential. This equation satisfies de unitarity condition of Eq. (2).

If we set the on-shell conditions $P \cdot p = P \cdot k = 0$ we have a closed three dimensional equation for the amplitudes ²⁷.

D. Lippmann-Schwinger Equation

The Lippmann-Schwinger equation has been employed recently Ref. [8] in successfully describing s -wave meson-meson scattering using a coupled channel formalism²⁸. This approach is also related to ours, although the way they obtain some results is not fully unproblematic. The authors of that reference compute the q^0 integral first, assuming that the contour can be closed at infinity, which for regular potentials and amplitudes may be acceptable. Then they introduce a three-momentum cut-off, hence breaking Lorentz and chiral invariance, and obtaining a three dimensional two body equation in the CM frame. Though this seems convenient for practical calculations, the justification for choosing this particular frame to include the cut-off is doubtful. Similarly to us, they also find that off-shellness may be ignored but it is not clear why chiral symmetry seems to play no role, particularly because their cut-off breaks it. In addition, to justify why the off-shellness can be ignored, they stick just to the one loop approximation. In our case we fully rely on the divergence structure of the non-linear sigma model, to all orders in the loop expansion, and on its chiral symmetric structure and make use of the chirally symmetric dimensional regularization to establish that the off-shellness can effectively be incorporated as a renormalization of the two particle irreducible amplitude.

Finally, in their finite cut-off framework they get the renormalization constant C_{00} and all higher order low-energy parameter contribution to this channel, as a specific function of the cut-off. That function should be the same for all isospin-angular momentum channels. This introduces undesired correlations between the higher order corrections in different channels

²⁷ We have the formula $d^4q = \frac{1}{2} \sqrt{(\hat{P} \cdot q)^2 - q^2} dq^2 d(\hat{P} \cdot q) d^2\hat{q}$, where $\hat{q}^2 = -1 = -\hat{P}^2$ and $P \cdot \hat{q} = 0$.

²⁸ Actually, their equation is the BSE, but we comply with their own notation.

which violates the spirit of ChPT. As a matter of fact, to reproduce the ρ -resonance within their framework requires a cut-off about three orders of magnitude bigger than that used in the σ -channel. We have already illustrated this point in Sect. V after Eq. (116). There, we compute the C parameter for the special case of dimensional regularization, but the discussion is identical if a three dimensional cut-off regularization is considered (see Eqs. (A3)-(A8) in the second item of Ref. [9]).

E. Inverse Amplitude Method

Eq. (65) provides an exact solution for the $\pi\pi$ elastic scattering amplitude, thus it is not fully surprising that the IAM of Ref. [4] can be rederived from it. The essential point is our lack of knowledge on the two particle irreducible amplitude, V_{IJ} , and the type of expansion proposed for it. For simplicity, let us consider the ρ -channel ($I = J = 1$). In this channel, we showed in Subsect. IV E that if the C_{11} parameter is set to zero, the potential V_{11} has to diverge before the resonance energy is reached. That makes hopeless a perturbative expansion for V_{11} , but it suggests an expansion for $1/V_{11}$, which should be small. Thus, expanding $1/V_{IJ}$ (we come back to the general case IJ) in powers of $1/f^2$ in Eq. (76), we get

$$T_{IJ}^{-1}(s)|_{\text{IAM}} = f^2[T_{IJ}^{(2)}(s)]^{-1} - T_{IJ}^{(4)}(s)[T_{IJ}^{(2)}(s)]^{-2} + \dots = -\bar{I}_0(s) + \frac{1}{V_{IJ}^{\text{IAM}}(s)} \quad (133)$$

where the C_{11} constant cancels out to all orders and $V(s)_{IJ}^{\text{IAM}} = T_{IJ}^{(2)}/(f^2 - \tau_{IJ}^{(4)}/T_{IJ}^{(2)})$. If $T_{IJ}^{(2)}$ has a single non-kinematical Adler zero, like for s -wave scattering, then this zero becomes a double one at the first order of the approximation, since $T = (T^{(2)})^2/(f^2 T^{(2)} - T^{(4)})$. In other words, T^{-1} has a double pole, in contradiction with the dispersion relation for the inverse scattering amplitude, Eq. (123), as pointed out in Ref. [6]. Notice that in the BSE the order of the Adler zero is always preserved. If in a particular channel, a resonance does not exist, one should expect $1/V$ not to be necessarily small and therefore the IAM might present some limitations. In our BSE framework, a chiral expansion of V is performed. Thanks to the inclusion of the renormalization parameter C , V might remain reasonably small in a wide region of energies. Besides, this scenario also allows us to compute form-factors.

F. Pade Approximants

In the Pade method [2], the series expansion in $1/f^2$ of the amplitude,

$$T_{IJ}(s) = T_{IJ}^{(2)}(s)/f^2 + T_{IJ}^{(4)}(s)/f^4 + T_{IJ}^{(6)}(s)/f^6 + \dots \quad (134)$$

truncated at some finite order, $2N$, is rewritten as a rational representation,

$$T_{IJ}(s) \approx T_{IJ}^{[2N-2K, 2K]}(s) = \frac{P_{IJ}^{2N-2K}(s)}{Q_{IJ}^{2K}(s)} \quad (135)$$

where $K = 0, \dots, N$, $P_{IJ}^{2N-2K}(s)$ and $Q_{IJ}^{2K}(s)$ are polynomials in $1/f^2$ of degrees $2N - 2K$ and $2K$ respectively. This approximation is enforced to reproduce the series expansion

for the amplitude and also to satisfy the unitarity condition, Eq. (26). For the particular case $2N = 4$, the only acceptable Pade approximant is the $[2, 2]$, and the IAM method is recovered. As we have already mentioned single non-kinematical Adler zeros are transformed at this level of approximation into double ones. In the language of the BSE, the Pade method is translated as a Pade approximant for the potential, for instance the $[2, 2]$ approximant would be

$$V_{IJ}^{[2,2]} = \frac{\frac{m^2}{f^2} [V_{IJ}^{(2)}(s)]^2}{V_{IJ}^{(2)}(s) - \frac{m^2}{f^2} V_{IJ}^{(4)}(s)} \quad (136)$$

which thanks to Eqs. (65) and (74) exactly yields to Eq.(133).

G. N/D Method

In the N/D method one starts with the dispersion relation for the partial wave scattering amplitude [54] (dropping the labels I, J for simplicity),

$$T(s) = B(s) + \frac{1}{\pi} \int_{4m^2}^{\infty} ds' \frac{T(s') \rho(s') T^*(s')}{s - s'} \quad (137)$$

where $\rho(s)$ was defined in Eq. (120) and $\text{Disc}[B(s)] = 0$ for $s > 4m^2$. $B(s)$ presents a discontinuity for $s < 0$. The method is based on the following assumptions: $T(s) = N(s)D(s)^{-1}$ and the discontinuity conditions

$$\begin{aligned} \text{Disc}[N(s)] &= D(s) \text{Disc}[T(s)] = D(s) \text{Disc}[B(s)] & s < 0 \\ \text{Disc}[D(s)] &= N(s) \text{Disc}[T^{-1}(s)] = -N(s)2i\rho(s) & s > 4m^2 \end{aligned} \quad (138)$$

Dispersion relations for $D(s)$ and $N(s)$ with suitable subtractions determine the full amplitude solely in terms of the left hand cut discontinuity. The point here is that the discontinuity conditions in Eq. (138) do not determine uniquely the amplitude, as it also happened in the approach presented in Subsect. VIB. Thus, one should supplement the discontinuity conditions with further information if possible. For instance the existence and position of the CDD (Castillejo, Dalitz and Dyson) poles [55], as recently invoked in Ref. [50] for meson-meson scattering, or of the bound states might help to find a physical solution from the whole family of solutions which satisfy the above discontinuity conditions. In any case, however, the multiplicative structure of the left and right hand cuts implied by the N/D method seems to contradict the additive cut structure deduced at two loops [34,35,56]. A more detailed study of the advantages and limitations of a N/D approach in this context will be presented elsewhere [57]. We note here, that the BSE preserves that additive left and right hand cuts, and hence a direct comparison with standard ChPT becomes possible.

VII. CONCLUSIONS

In this paper we have studied the consequences of chiral symmetry for $\pi\pi$ scattering and also for the scalar and vector form factors within an approach based on the BSE. Besides the

automatic incorporation of elastic unitarity, it becomes clear what is the subset of diagrams which is summed up. This requires the identification of a *potential* which corresponds to the amputated two particle irreducible Green function. As such, the identification is not unique, leaving room for a scale ambiguity, or equivalently a subtraction constant in the language of dispersion relations. We have dealt with the issue of renormalizability of the BSE within the framework of ChPT. We have recognized two alternative extreme viewpoints to implement the renormalization program which we have named: off-shell and on-shell schemes.

In the off-shell scheme, the off-shell dependence of the potential is kept while solving the BSE. This way of proceeding allows to choose a renormalization scheme where the finite parts of the ultraviolet power divergences are not set to zero. This, still, produces more constants than those allowed by crossing at a given order in the chiral expansion, and it becomes sensible to fine tune them in a way to comply as best as we can with the crossing symmetry requirement. In practice we have found it convenient to implement this as a restriction on our partial wave amplitudes by matching those to Taylor expansions of the ChPT ones, including the contribution of the left hand cut. This off-shell scheme is rather simple at the lowest approximation level, and at the same time allows for a satisfactory fit to the phase shift $\pi\pi$ scattering data in the $I = 0, 1, 2$ and $J = 0, 1$ channels leading to a prediction of the low energy parameters $\bar{l}_{1,2,3,4}$ with varying degree of accuracy [12]. Conversely, using commonly accepted values for the $\bar{l}_{1,2,3,4}$ with their error-bars, a satisfactory and compatible prediction of the scattering data is achieved. In particular, our extrapolation of the low energy standard ChPT phase shifts in the $I = J = 1$ channel to higher energies predicts the correct ρ meson mass and width with 10% and 25% accuracy respectively. This approach, although very efficient to describe the data in the different isospin channels, becomes very cumbersome to pursue at next to leading order.

Thus, we have also considered the on-shell scheme. As discussed in the paper, the fact that we are dealing with an EFT provides interesting insight into the problem. Given the infinite number of counter-terms necessary to ensure the renormalizability of the theory in a broad sense, one can reorganize the summation of diagrams in a way as to include in the potential the unknown coefficients. As an important consequence, a dramatic simplification in the solution of the BSE arises: all the divergences originated by the off-shell behavior of the potential can be effectively renormalized by redefining the potential and simultaneously ignoring the off-shellness in the solution of the BSE. In particular, on shell information for the full scattering amplitude can simply be obtained from the on-shell potential with unknown coefficients. We have found the on-shell scheme more convenient to take advantage of the ChPT information to one and two loops than the off-shell scheme. Eventually, both schemes would become equivalent if the *exact* amplitude were considered.

In particular, by using the on-shell scheme we have constructed a $\pi\pi$ amplitude, which exactly reproduces the tree plus one loop scattering amplitude of ChPT and embodies exact elastic unitarity to all orders in the chiral expansion parameter $1/f^2$. Thus, the definition of the phase shifts is unambiguous. In addition, a prediction for some ChPT two-loop low energy parameters can be also made. The BSE within the on-shell scheme proves particularly useful when dealing with the vector and scalar form factors. Watson's theorem is automatically satisfied without explicitly invoking an Omnès representation. The requirement of an asymptotic behavior compatible with a once subtracted dispersion relation yields to a unambiguous prediction for the form factors, with no more undetermined constants than

those suggested by standard ChPT. Equipped with all this formalism we have been able to make a very accurate determination, in terms of estimated errors, of some low energy parameters. In particular, a remarkably accurate prediction has been achieved for the difference $\bar{l}_1 - \bar{l}_2$ and the parameter \bar{l}_6 by fitting the vector form factor, rather than the $\pi\pi$ scattering amplitude in the vector-isovector channel. Predictions for the corresponding δ_{11} phase shift with the propagated errors are satisfactory and accurate from threshold up to 1200 MeV. Similar features are also found for other channels, although there the maximum energy, for which the predictions with their error-bars apply, ranges from 600 MeV in the scalar-isoscalar, to 1400 MeV in the scalar-isotensor channel. d -waves corresponding to the $I = 0$ and 2 channels are also describable up to 1000 MeV. In all cases we observe that the higher the energy the larger the error bars. This is not surprising since, our unitary amplitudes are generated from low energy information.

From the point of view of predictive power we have also undertaken a thorough analysis of the predictions for the $\mathcal{O}(1/f^6)$ contributions of the amplitudes to the threshold parameters, as compared to standard ChPT two-loop ones under a resonance saturation hypothesis [35]. The level of prediction is never less accurate than in the case of ChPT, and in some cases it is much better. The total predictions for the effective range parameters are in agreement with the experimental values within errors.

The present calculation can be improved and extended in several ways which we describe in the following. First of all, the formalism presented in this paper can be enlarged to include coupled channel contributions. All of our formulae are valid for a coupled channel scenario just bearing in mind that now one is dealing with matrices instead of commuting \mathbb{C} -numbers. This topic has been partially addressed in Sect. IV C. Secondly, our results, regarding the accurate description of one loop parameters with the present unitarization method, advises to implement the next order in our expansion. In this way we might try to determine, from fits to the data, more accurately some of the two loop parameters $b_{1,2,3,4,5,6}$, disposing the physically compelling, but unmotivated from a standard ChPT viewpoint, resonance saturation hypothesis. In this regard, the consideration of our formalism for describing K_{l_4} decays, in conjunction with the electric pion form factor might prove very fruitful in order to provide more accurate constraints for the one loop parameters. In neither case, have we addressed the determination of \bar{l}_5 , which is related to the pion polarizability, and would require a thorough analysis of Compton scattering on the pion. In this respect, there exist already attempts in the literature trying to describe the physical process, but never focused from the point of view of determining this parameter. We leave these points for future research.

ACKNOWLEDGMENTS

We would like to acknowledge useful discussions with J.A. Oller, E. Oset and L.L. Salcedo. This research was supported by DGES under contract PB98-1367 and by the Junta de Andalucía.

APPENDIX A: DETAILS ON THE OFF-SHELL BSE SCHEME

1. I=0 $\pi\pi$ scattering

The ansatz of Eq. (17) reduces the BSE to the linear algebraic system of equations

$$\begin{aligned}
 A &= \frac{5m^2 - 3s}{2f^2} + \frac{(5m^2 - 3s)I_0(s) - 2I_2(s)}{2f^2} A + \frac{(5m^2 - 3s)I_2(s) - 2I_4(s)}{2f^2} B \\
 B &= -\frac{1}{f^2} - \frac{AI_0(s) + BI_2(s)}{f^2} \\
 B &= -\frac{1}{f^2} + \frac{(5m^2 - 3s)I_0(s) - 2I_2(s)}{2f^2} B + \frac{(5m^2 - 3s)I_2(s) - 2I_4(s)}{2f^2} C \\
 C &= -\frac{BI_0(s) + CI_2(s)}{f^2}
 \end{aligned} \tag{A1}$$

as we see there are four equations and three unknowns. For the system to be compatible necessarily one equation ought to be linearly dependent. This point can be verified by direct solution of the system. The integrals appearing in the previous system are of the form

$$I_{2n}(s) = i \int \frac{d^4q}{(2\pi)^4} \frac{(q^2)^n}{[q_-^2 - m^2 + i\epsilon][q_+^2 - m^2 + i\epsilon]} \tag{A2}$$

$I_0(s)$, $I_2(s)$ and $I_4(s)$ are logarithmically, quadratically and quartically ultraviolet divergent integrals. Translational and Lorentz invariance relate the integrals $I_2(s)$ and $I_4(s)$ with $I_0(s)$ and the divergent constants $I_2(4m^2)$ and $I_4(4m^2)$.

$$\begin{aligned}
 I_0(s) &= I_0(4m^2) + \bar{I}_0(s) \\
 I_2(s) &= (m^2 - s/4)I_0(s) + I_2(4m^2) \\
 I_4(s) &= (m^2 - s/4)^2 I_0(s) + I_4(4m^2)
 \end{aligned} \tag{A3}$$

Note also that $I_0(s)$ is only logarithmically divergent and it only requires one subtraction, i.e., $\bar{I}_0(s) = I_0(s) - I_0(4m^2)$ is finite and it is given by

$$\bar{I}_0(s) = \frac{1}{(4\pi)^2} \sqrt{1 - \frac{4m^2}{s}} \log \frac{\sqrt{1 - \frac{4m^2}{s}} + 1}{\sqrt{1 - \frac{4m^2}{s}} - 1} \tag{A4}$$

where the complex phase of the argument of the log is taken in the interval $[-\pi, \pi]$. Using the relations of Eq. (A3) in the solution of the linear system of Eq. (A1) we get

$$\begin{aligned}
 A(s) &= \frac{1}{D(s)} \left[\frac{5m^2 - 3s}{f^2} + \frac{I_4(4m^2) + (m^2 - s/4)^2 I_0(s)}{f^4} \right] \\
 B(s) &= \frac{-1}{D(s)} \left[\frac{1}{f^2} + \frac{I_2(4m^2) + (m^2 - s/4)I_0(s)}{f^4} \right] \\
 C(s) &= \frac{1}{D(s)} \frac{I_0(s)}{f^4}
 \end{aligned} \tag{A5}$$

where,

$$D(s) = \left[1 + \frac{I_2(4m^2)}{f^2}\right]^2 + I_0(s) \left(\frac{2s - m^2}{2f^2} - \frac{(s - 4m^2)I_2(4m^2) + 2I_4(4m^2)}{2f^4}\right) \quad (\text{A6})$$

Eqs. (A5) and (A6) require renormalization, we will address this issue in Subsect. III D.

2. $I=1$ $\pi\pi$ scattering

The full off-shell scattering amplitude solution of the BSE in this channel is given by the ansatz of Eq. (20) with the functions M and N given by

$$\begin{aligned} M(s) &= \frac{2}{f^2} \left(1 - \frac{2I_2(4m^2) + (4m^2 - s)I_0(s)}{6f^2}\right)^{-1} \\ sN(s) &= \frac{M(s)}{6f^2} \frac{4I_2(4m^2) - (4m^2 - s)I_0(s)}{1 - I_2(4m^2)/f^2} \end{aligned} \quad (\text{A7})$$

To obtain Eq. (A7) we have used that

$$\begin{aligned} I^{\mu\nu}(s) &= i \int \frac{d^4q}{(2\pi)^4} q^\mu q^\nu \Delta(q_+) \Delta(q_-) \\ &= \frac{1}{3} \left(g^{\mu\nu} - \frac{P^\mu P^\nu}{s}\right) \left[(m^2 - s/4)I_0(s) - I_2(4m^2)\right] + \frac{1}{2} g^{\mu\nu} I_2(4m^2) \end{aligned} \quad (\text{A8})$$

3. $I=2$ $\pi\pi$ scattering

The functions A, B and C entering in the amplitude of Eq. (23) can be determined by solving the BSE in this channel, and thus we find

$$\begin{aligned} A(s) &= \frac{1}{D(s)} \left[\frac{m^2}{f^2} + \frac{I_4(4m^2) + (m^2 - s/4)^2 I_0(s)}{f^4}\right] \\ B(s) &= \frac{-1}{D(s)} \left[\frac{1}{f^2} + \frac{I_2(4m^2) + (m^2 - s/4)I_0(s)}{f^4}\right] \\ C(s) &= \frac{1}{D(s)} \frac{I_0(s)}{f^4} \end{aligned} \quad (\text{A9})$$

where

$$D(s) = \left[1 + \frac{I_2(4m^2)}{f^2}\right]^2 + I_0(s) \left[\frac{2m^2 - s}{2f^2} - \frac{(s - 2m^2)I_2(4m^2) + 2I_4(4m^2)}{2f^4}\right] \quad (\text{A10})$$

Once again Eqs. (A9) and (A10) require renormalization, we will get back to this point in Subsect. III D.

4. On-shell and off-shell unitarity

Off-shell unitarity (Eq. (2)) imposes a series of conditions to be satisfied by the amplitudes obtained in the previous subsections. Those read for the $I = 1$ case

$$\begin{aligned}\text{Disc}[N(s)] &= \frac{(s - 4m^2)}{12} |N(s)|^2 \text{Disc}[I_0(s)] \\ \text{Disc}[M(s)] &= -\frac{\text{Disc}[N(s)]}{s}\end{aligned}\tag{A11}$$

and for the $I = 0, 2$ cases, they are

$$\begin{aligned}\text{Disc}[A(s)] &= -\left|A(s) + B(s)(m^2 - s/4)\right|^2 \text{Disc}[I_0(s)] \\ \text{Disc}[C(s)] &= -\left|B(s) + C(s)(m^2 - s/4)\right|^2 \text{Disc}[I_0(s)] \\ \text{Disc}[B(s)] &= \left((m^2 - s/4)B(s) + A(s)\right)^* \left((m^2 - s/4)C(s) + B(s)\right) \text{Disc}[I_0(s)]\end{aligned}\tag{A12}$$

where $\text{Disc}[f(s)] \equiv f(s + i\epsilon) - f(s - i\epsilon)$, $s > 4m^2$.

On the other hand and thanks to the Schwartz's Reflex ion Principle, $\text{Disc}[I_0(s)]$ is given by

$$\begin{aligned}\text{Disc}[I_0(s)] &\equiv I_0(s + i\epsilon) - I_0(s - i\epsilon) = 2i\text{Im}\bar{I}_0(s + i\epsilon) \\ &= -i(2\pi)^2 \int \frac{d^4q}{(2\pi)^4} \delta^+(q_+^2 - m^2) \delta^+(q_-^2 - m^2) = -\frac{i}{8\pi} \sqrt{1 - \frac{4m^2}{s}}, \quad s > 4m^2\end{aligned}\tag{A13}$$

5. Renormalization method, crossing symmetry and lagrangian counter-terms

The method of subtraction integrals makes any amplitude finite, by definition. In customary renormalizable theories or EFT's, one can prove in perturbation theory (where crossing is preserved order by order) that this method has a counter-term interpretation. This is traditionally considered a test for a local theory, from which microcausality follows. Since we are violating crossing it is not clear whether or not our renormalization method admits a Lagrangian interpretation beyond the actual level of approximation. These are in fact a sort of integrability conditions; the renormalized amplitudes should be indeed functional derivatives of the renormalized Lagrangian. It is actually very simple to see that these conditions are violated by our solution. In terms of the generating functional $Z[J]$ the four point renormalized Green's function is defined as

$$\begin{aligned}\langle 0|T\{\pi_a(x_1)\pi_b(x_2)\pi_c(x_3)\pi_d(x_4)\}|0\rangle &= \frac{1}{Z[J]} \frac{\delta^4 Z[J]}{\delta J_a(x_1)\delta J_b(x_2)\delta J_c(x_3)\delta J_d(x_4)} \Big|_{J=0} = \\ &\int \frac{d^4k}{(2\pi)^4} \frac{d^4p}{(2\pi)^4} \frac{d^4P}{(2\pi)^4} \frac{d^4P'}{(2\pi)^4} e^{ip(x_1-x_2)} e^{ik(x_4-x_3)} e^{iP(x_1+x_2)/2} e^{-iP'(x_3+x_4)} \Delta_{aa'}(p_+) \\ &\times \Delta_{bb'}(p_-) (-i)T_P(p, k)_{a'b';c'd'} \delta^4(P - P') \Delta_{cc'}(k_+) \Delta_{dd'}(k_-)\end{aligned}\tag{A14}$$

The integrability conditions are simply the equivalence between crossed derivatives which, as one clearly sees, implies in particular the crossing condition for the scattering amplitude. Since crossing is violated, the integrability conditions are not fulfilled and hence our renormalized amplitude does not derive from a renormalized Lagrangian.

Crossing symmetry can be restored, in certain approximation, as it is discussed in Subsect. III E, by imposing suitable constraints between the subtraction constants which appear in the renormalization scheme described in Subsect. III D. These conditions reads:

$$\begin{aligned}
75I_2^{R,I=0}/2m^2 + 8I_0^{R,I=1} + 33I_0^{R,I=0} + 5I_2^{R,I=1}/m^2 + \frac{10157}{1920\pi^2} &= 0 \\
I_0^{R,I=2} - \frac{4I_0^{R,I=1}}{15} - \frac{8I_0^{R,I=0}}{5} - \frac{719}{7200\pi^2} &= 0 \\
\frac{I_2^{R,I=2}}{4m^2} + \frac{4(I_0^{R,I=1} + I_0^{R,I=0})}{25} + \frac{I_2^{R,I=1}}{12m^2} + \frac{887}{36000\pi^2} &= 0 \\
\frac{I_4^{R,I=2}}{16m^4} + \frac{17I_0^{R,I=1}}{500} + \frac{111I_0^{R,I=0}}{4000} + \frac{3I_2^{R,I=1}}{200m^2} - \frac{I_4^{R,I=0}}{40m^4} + \frac{2159}{480000\pi^2} &= 0 \tag{A15}
\end{aligned}$$

The first of these relations was obtained in Ref. [12].

Finally and for the sake of clarity we quote here the result of inverting the Eq. (18) of Ref. [12],

$$\begin{aligned}
I_0^{R,I=1} &= -\frac{1}{16\pi^2} (2(\bar{l}_2 - \bar{l}_1) + 97/60) \\
I_2^{R,I=1} &= \frac{m^2}{8\pi^2} ((2(\bar{l}_2 - \bar{l}_1) + 3\bar{l}_4 - 65/24)) \\
I_0^{R,I=0} &= -\frac{1}{576\pi^2} (22\bar{l}_1 + 28\bar{l}_2 + 31/2) \\
I_4^{R,I=0} &= \frac{m^4}{7680\pi^2} (-172\bar{l}_1 - 568\bar{l}_2 + 600\bar{l}_3 - 672\bar{l}_4 + 1057) \tag{A16}
\end{aligned}$$

6. Remarks on the choice of the pion field

The solution of the BSE requires an ansatz for the off-shell potential $V_P(p, k)$. The non-linear realization of chiral symmetry through the non-linear σ -model posses an additional difficulty. The pion field, $\vec{\phi}$, is encoded in the unitary space-time matrix $U(x)$, $U^\dagger U = 1$, so it lives in the three sphere of radius f . However, the particular set of coordinates is not unique. For instance, one may have a *polar* representation $U(x) = e^{i\vec{\phi}\cdot\vec{\tau}/f}$, being $\vec{\tau}$ the Pauli matrices, a *cartesian* representation $U(x) = \sqrt{1 - \vec{\phi}^2/f^2} + i\vec{\phi}\cdot\vec{\tau}/f$, or a *stereographic* representation $U(x) = (1 + i\vec{\phi}\cdot\vec{\tau}/2f)/(1 - i\vec{\phi}\cdot\vec{\tau}/2f)$. It is well known that any representation yields to the same kinetic and mass terms, but different pion interaction terms. Indeed, up to second order in the chiral expansion, the effective lagrangian reads

$$\mathcal{L} = \frac{f^2}{4} \text{tr}(\partial^\mu U^\dagger \partial_\mu U) + \frac{f^2 m^2}{4} \text{tr}(U + U^\dagger - 2) \tag{A17}$$

which up to fourth order in the pion field becomes

$$\mathcal{L} = \frac{1}{2}(\partial_\mu \vec{\phi})^2 - \frac{m^2}{2}\vec{\phi}^2 - \frac{\alpha}{4f^2}(\partial_\mu \vec{\phi})^2 \vec{\phi}^2 + \frac{1-\alpha}{2f^2}(\vec{\phi} \partial_\mu \vec{\phi})^2 + (\alpha - \frac{1}{2})\frac{m^2}{4f^2}\vec{\phi}^4 \quad (\text{A18})$$

where the unfixed α parameter has its origin in the arbitrariness on the form of the U -matrix. Thus, the polar and cartesian representations correspond to $\alpha = 0$ whereas the stereographic representation leads to $\alpha = 1$. The α dependence disappears if one uses the equation of motion. The above Lagrangian gives

$$A_P(p, k) = -\frac{1}{f^2} \left\{ s \left(1 - \frac{\alpha}{2} \right) - \alpha (p^2 + k^2) + m^2 (2\alpha - 1) \right\} \quad (\text{A19})$$

which by means of the symmetry properties discussed in Sect. II completely defines the two identical isovector (off- or on-shell) meson scattering amplitude $(T_P(p, k)_{ab;cd})$ for the process $(P/2 + p, a) + (P/2 - p, b) \rightarrow (P/2 + k, c) + (P/2 - k, d)$, defined in Eq. (3). On the mass-shell the dependence on α of the amplitude disappears. Off the mass shell an explicit α dependence is exhibited. Thus, the BSE kernel $V_P(p, k)$ will depend on α and might generate also an α -dependence in the solutions of the BSE. For on-shell pion scattering and when the exact potential V and propagator Δ are used the α dependence drops out. However, when approximated V and Δ are inserted in the BSE, the solution of the equation might display an α dependence, even for on-shell pions. This is the case for the lowest order $I = 0$ and $I = 2$ on-shell solutions,

$$T_{00}^{-1}(s) = -I_0(s) + \frac{2(f^2 + (1 - 5\alpha/2)I_2(4m^2))^2}{(m^2 - 2s)f^2 + (1 - 5\alpha/2)^2(2I_4(4m^2) + (s - 4m^2)I_2(4m^2))} \quad (\text{A20})$$

$$T_{20}^{-1}(s) = -I_0(s) + \frac{2(f^2 + (1 - \alpha)I_2(4m^2))^2}{(s - 2m^2)f^2 + (1 - \alpha)^2(2I_4(4m^2) + (s - 4m^2)I_2(4m^2))} \quad (\text{A21})$$

where both amplitudes above require renormalization and reduce to those given in Eqs. (18) and Eqs. (24) for $\alpha = 0$. The lowest order $I = 1$ BSE solution turns out to be independent of α .

It is worth noticing that the energy dependence encoded in the amplitudes above is not changed by this α dependence, and they can generically be written as

$$T_{00(20)}^{-1}(s) = -\bar{I}_0(s) - c + \frac{1}{a + bs} \quad (\text{A22})$$

with a , b and c suitable constants. So there is redundancy of parameters, since we have four parameters $I_0(4m^2)$, $I_2(4m^2)$, $I_4(4m^2)$ and α , mapped into three parameters a, b and c . Obviously, the particular value of α would be irrelevant, when a fit of these constants to data is performed, as it was done in Ref. [12]. The trouble might appear, as we will see, when matching these amplitudes to those deduced in ChPT, which of course do not present any dependence on α for pions on the mass shell.

The α dependence shown in Eqs. (A20) and (A21) is undesirable because we are dealing to on-shell amplitudes. It appears because we have not generated loops in the t - and u -channels, i.e. the amplitudes do not satisfy exact crossing. On the light of this discussion, we envisage two alternative procedures linked to different renormalization schemes:

- Within the renormalization scheme presented in Sect. IIID, we can match the $1/f^2$ expansion of the BSE amplitude up to $\mathcal{O}(1/f^4)$, to the threshold expansion, up to order $(s-4m^2)^2$, of the Gasser-Leutwyler amplitudes, as it has been done in Sect. A 5. This procedure modifies the last of Eqs. (A16) and all of the constraints of Eq. (A15), and ensures the α independence of the matched terms, but there remains a residual α dependence in the renormalized on-shell BSE amplitude, starting at order $\mathcal{O}(1/f^6)$. Actually, this matching procedure does not work if $\alpha = 2$ or $\alpha = -1$, because in these cases the BSE coefficients of $(s-4m^2)/f^4$ and $(s-4m^2)^2/f^4$ pieces are not independent for $I = 0$ and $I = 2$ respectively, making then the matching to the Gasser-Leutwyler amplitudes overdetermined²⁹. In addition, we do not have any restriction on the possible α values. This is way we find more appropriate the following scheme.
- From the renormalization discussion presented in Sect. IIID it is clear, as it is also the case in standard ChPT, that to achieve renormalization of the amplitudes an infinite number of counter-terms is required. Being then the finite parts, order by order in the perturbative expansion, undetermined and have to be either fitted to data or determined from the underlying QCD dynamics. This implies in particular that the divergent integrals appearing in the numerator and denominator in Eqs. (A20) and (A21) may be chosen to be independent of each other. This can be used advantageously to eliminate the explicit α dependence, by simply redefining the integrals, $I_2(4m^2)(1-5\alpha/2) \rightarrow I_2(4m^2)$, $I_2(4m^2)(1-\alpha) \rightarrow I_2(4m^2)$ in the numerators of Eqs. (A20) and (A21), and $I_{2,4}(4m^2)(1-5\alpha/2)^2 \rightarrow I_{2,4}(4m^2)$, $I_2(4m^2)(1-\alpha)^2 \rightarrow I_2(4m^2)$ in the denominators of Eqs. (A20) and (A21), respectively, since we know that the total amplitude must be α independent. Even though this choice might appear more arbitrary than the scheme presented in Sect. IIID, it is still more restrictive than what the renormalization of an EFT allows for.

From the discussion above, we prefer to work within the second scenario where the unphysical α -dependence can be ignored, when looking at on-shell amplitudes, and the particular value $\alpha = 0$ can be considered, as we have done along Sect. III. Within this renormalization scheme any value of α would lead to the same results presented in that section.

APPENDIX B: LEADING AND NEXT-TO-LEADING ELASTIC $\pi\pi$ SCATTERING AMPLITUDES IN CHPT

The $\mathcal{O}(p^2) + \mathcal{O}(p^4)$ on-shell $SU(2)$ -ChPT elastic $\pi\pi$ amplitudes, expressed in terms of the renormalization invariant parameters $\bar{l}_{1,2,3,4}$, are given³⁰ by [16]

²⁹That would require a restriction among the \bar{l} 's.

³⁰Note that the function $\bar{I}_0(s)$, fulfilling $\bar{I}_0(4m^2) = 0$ is related to that of [16] fulfilling $\bar{J}(0) = 0$ by

$$T_{IJ}(s) = T_{IJ}^{(2)}(s)/f^2 + T_{IJ}^{(4)}(s)/f^4 \quad (\text{B1})$$

$$T_{IJ}^{(4)}(s) = \tau_{IJ}^{(4)}(s) + \bar{I}_0(s) \times [T_{IJ}^{(2)}(s)]^2 \quad (\text{B2})$$

$$T_{IJ}^{(2)}(s) = \begin{cases} \frac{m^2-2s}{2} & I = 0; J = 0 \\ 0 & I = 0; J = 2 \\ \frac{4m^2-s}{6} & I = 1; J = 1 \\ \frac{s-2m^2}{2} & I = 2; J = 0 \\ 0 & I = 2; J = 2 \end{cases} \quad (\text{B3})$$

$$\tau_{IJ}^{(4)}(s) = -\frac{1}{192\pi^2}g_{IJ} + \frac{1}{12}h_{IJ} \quad (\text{B4})$$

$$h_{IJ} = \frac{1}{2} \int_{-1}^1 d(\cos \theta) \left(f_I(t)\bar{I}_0(t) + f_I(u)\bar{I}_0(u) \right) P_J(\cos \theta)$$

$$= \begin{cases} \frac{5m^4}{4\pi^2} + \frac{101m^2(s-4m^2)}{96\pi^2} + \frac{191(s-4m^2)^2}{288\pi^2} + \dots & I = 0; J = 0 \\ \frac{287(s-4m^2)^2}{2880\pi^2} + \frac{481(s-4m^2)^3}{67200m^2\pi^2} \dots & I = 0; J = 2 \\ \frac{89m^2(s-4m^2)}{288\pi^2} - \frac{37(s-4m^2)^2}{2880\pi^2} + \dots & I = 1; J = 1 \\ \frac{11m^4}{4\pi^2} + \frac{179m^2(s-4m^2)}{96\pi^2} + \frac{769(s-4m^2)^2}{1440\pi^2} + \dots & I = 2; J = 0 \\ \frac{529(s-4m^2)^2}{14400\pi^2} + \frac{277(s-4m^2)^3}{67200m^2\pi^2} + \dots & I = 2; J = 2 \end{cases} \quad (\text{B5})$$

where $t = -2(\frac{s}{4} - m^2)(1 - \cos \theta)$, $u = -2(\frac{s}{4} - m^2)(1 + \cos \theta)$ and

$$f_I(x) = \begin{cases} 10x^2 + x(2s - 32m^2) + 37m^4 - 8sm^2 & I = 0 \\ 2x^2 + x(s + 2m^2) - m^4 - 4sm^2 & I = 1 \\ 4x^2 - x(s + 2m^2) - 5m^4 + 4sm^2 & I = 2 \end{cases} \quad (\text{B6})$$

$$\bar{I}_0(s) = -\bar{J}(s) + \frac{1}{8\pi^2}$$

$$g_{IJ} = \begin{cases} m^4 (40\bar{l}_1 + 80\bar{l}_2 - 15\bar{l}_3 + 84\bar{l}_4 + 125) + m^2(s - 4m^2) \times \\ \quad (32\bar{l}_1 + 48\bar{l}_2 + 24\bar{l}_4 + \frac{232}{3}) + (s - 4m^2)^2 (\frac{22}{3}\bar{l}_1 + \frac{28}{3}\bar{l}_2 + \frac{142}{9}) & I = 0; J = 0 \\ \frac{2(s-4m^2)^2}{15} (\bar{l}_1 + 4\bar{l}_2 + \frac{16}{3}) & I = 0; J = 2 \\ \frac{s-4m^2}{3} [4m^2 (-2\bar{l}_1 + 2\bar{l}_2 + 3\bar{l}_4 + 1) + (s - 4m^2) (-2\bar{l}_1 + 2\bar{l}_2 + 1)] & I = 1; J = 1 \\ m^4 (16\bar{l}_1 + 32\bar{l}_2 - 6\bar{l}_3 - 24\bar{l}_4 + 50) + m^2(s - 4m^2) \times \\ \quad (8\bar{l}_1 + 24\bar{l}_2 - 12\bar{l}_4 + \frac{100}{3}) + (s - 4m^2)^2 (\frac{4}{3}\bar{l}_1 + \frac{16}{3}\bar{l}_2 + \frac{64}{9}) & I = 2; J = 0 \\ \frac{2(s-4m^2)^2}{15} (\bar{l}_1 + \bar{l}_2 + \frac{11}{6}) & I = 2; J = 2 \end{cases} \quad (\text{B7})$$

The integrals which appear in the definition of h_{IJ} in Eq. (B4) can be done analytically by means of the change of variables:

$$\cos \theta \rightarrow x = \frac{\sqrt{1 - \frac{4m^2}{\xi(\cos \theta)}} + 1}{\sqrt{1 - \frac{4m^2}{\xi(\cos \theta)}} - 1} \quad (\text{B8})$$

being $\xi(\cos \theta) = t$ or u . Thus we get,

$$h_{IJ}(s) = a_{IJ}(s) + b_{IJ}(s)L(s) + c_{IJ}(s)L(s)^2 \quad (\text{B9})$$

where

$$L(s) = \log\left(\frac{1 + \sqrt{1 - \frac{4m^2}{s}}}{1 - \sqrt{1 - \frac{4m^2}{s}}}\right) \quad (\text{B10})$$

and $s > 4m^2$. In the following we list some special cases of interest,

$$\begin{aligned} a_{00} &= \frac{-506m^4 + 130m^2s - 11s^2}{144\pi^2} \\ b_{00} &= \frac{75m^4 - 40m^2s + 7s^2}{24\pi^2} \sqrt{\frac{s}{s - 4m^2}} \\ c_{00} &= \frac{m^4(25m^2 - 6s)}{8\pi^2(s - 4m^4)} \end{aligned} \quad (\text{B11})$$

$$\begin{aligned} a_{11} &= \frac{120m^6 - 149m^4s + 37m^2s^2 + s^3}{144\pi^2(s - 4m^2)} \\ b_{11} &= \frac{36m^6 - 72m^4s + 16m^2s^2 - s^3}{48\pi^2(s - 4m^2)} \sqrt{\frac{s}{s - 4m^2}} \\ c_{11} &= \frac{m^4(6m^4 + 13m^2s - 3s^2)}{8\pi^2(s - 4m^2)^2} \end{aligned} \quad (\text{B12})$$

$$\begin{aligned}
a_{20} &= \frac{308m^4 - 58m^2s - 25s^2}{288\pi^2} \\
b_{20} &= \frac{6m^4 - 32m^2s + 11s^2}{48\pi^2} \sqrt{\frac{s}{s - 4m^2}} \\
c_{20} &= \frac{m^4(m^2 + 3s)}{8\pi^2(s - 4m^2)}
\end{aligned} \tag{B13}$$

$$\begin{aligned}
a_{02} &= \frac{-31936m^8 + 27646m^6s - 4371m^4s^2 + 61m^2s^3 + 14s^4}{720\pi^2(s - 4m^2)^2} \\
b_{02} &= \frac{516m^8 - 760m^6s + 180m^4s^2 - 18m^2s^3 + s^4}{24\pi^2(s - 4m^2)^2} \sqrt{\frac{s}{s - 4m^2}} \\
c_{02} &= \frac{m^4(172m^6 - 98m^4s + 49m^2s^2 - 6s^3)}{8\pi^2(s - 4m^2)^3}
\end{aligned} \tag{B14}$$

$$\begin{aligned}
a_{22} &= \frac{124672m^8 - 48832m^6s + 53592m^4s^2 - 5182m^2s^3 + 247s^4}{14400\pi^2(s - 4m^2)^2} \\
b_{22} &= \frac{-480m^8 - 980m^6s + 117m^4s^2 - 36m^2s^3 + 2s^4}{120\pi^2(s - 4m^2)^2} \sqrt{\frac{s}{s - 4m^2}} \\
c_{22} &= -\frac{m^4(32m^6 - 76m^4s + 11m^2s^2 - 3s^3)}{8\pi^2(s - 4m^2)^3}
\end{aligned} \tag{B15}$$

-
- [1] S. Gasiorowicz, *Elementary Particle Physics*, Wiley (1966).
Many modern references can be traced from A. M. Bernstein, D. Drechsel and T. Walcher (eds.), *Chiral Dynamics: Theory and Experiment*, Lecture Notes in Physics, Springer (1998).
- [2] A. Dobado, M.J. Herrero and T.N. Truong, Phys. Lett. **B235** (1990) 134.
- [3] M. B. Einhorn, Nucl. Phys. **B246** (1984) 75; A. Dobado and J.R. Peláez, Phys. Lett. **B286** (1992) 136; A. Dobado and J. Morales, Phys. Rev. **D52** (1995) 2878.
- [4] A. Dobado and J.R. Peláez, Phys. Rev. **D47** (1993) 4883; T. Hannah, Phys. Rev. **D54** (1996) 4648; *ibidem* **D55** (1997) 5613.
- [5] J.S. Borges, J.S. Barbosa and V. Oguri, Phys. Lett. **B393** (1997) 413.
- [6] M. Boggione and M.R. Pennington, Z. Phys. **C75** (1997) 113.
- [7] G. Wanders, Phys. Rev. **D56** (1997) 4328; B. Ananthanarayan and P. Buttiker, Phys. Lett. **B415** (1997) 402; B. Ananthanarayan, Phys. Rev. **D58** (1998) 036002.
- [8] J.A. Oller and E. Oset, Nucl. Phys. **A620** (1997) 438.
- [9] J.A. Oller, E. Oset and J.R. Peláez, Phys. Rev. Lett. **80** (1998) 3452; *ibidem*, Phys. Rev. **D59** (1991) 074001.
- [10] H.A. Bethe and E.E. Salpeter, Phys. Rev. **82** (1951) 309; for a review see e.g. N. Nakanishi, Suppl. Prog. Theor. Phys., vol.**43** (1969) 1.
- [11] B. D. Keister and W. N. Polyzou, *Adv. Nucl. Phys.* **20** (1991) 225; J. W. Negele and E. Vogt (eds.).
- [12] J. Nieves and E. Ruiz Arriola, Phys. Lett. **B455** (1999) 30.
- [13] J.D. Bjorken and S. D. Drell, *Relativistic Quantum Fields* (1965) McGraw-Hill.
- [14] S.R. Beane and C.B. Chiu, hep-ph/9303254; S.R. Beane and S. Varma, Phys. Lett. **B313** (1993) 165.
- [15] See e.g. U. van Kolck, hep-ph/9711222, Nucl. Phys. **A645** (1999) 273; S.R. Beane, Acta Phys. Polon. **B29** (1998) 3161; D. Kaplan, nucl-th/9901003 and references therein.
- [16] J. Gasser and H. Leutwyler, Ann. of Phys., NY **158** (1984) 142.
- [17] J. Gasser and U.G. Meißner, Nucl. Phys. **B357** (1991) 90.
- [18] J. Bijnens, G. Colangelo and P. Talavera, JHEP **9805** (1998) 014.
- [19] C. Riggenbach, J.F. Donoghue, J. Gasser and B.R. Holstein, Phys. Rev. **D43** (1991) 127.
- [20] J. Bijnens, G. Colangelo and J. Gasser, Nucl. Phys. **B 427** (1994) 427.
- [21] S. D. Protopopescu *et. al.*, Phys. Rev. **D7** (1973) 1279.
- [22] B. Hyams, C.Jones and P. Weilhammer, Nucl. Phys. **B64** (1973) 134; W. Ochs, Thesis, Ludwig-Maximilians-Universität, 1973.
- [23] P. Estabrooks and A. D. Martin, Nucl. Phys. **B79** (1974) 301.
- [24] V. Srinivasan *et. al.*, Phys. Rev. **D12** (1975) 681.
- [25] L. Rosselet *et. al.*, Phys. Rev. **D15** (1977) 574.
- [26] R. Kaminski, L. Lesniak and K. Rybicki, Z. Phys. **C74** (1997) 79.
- [27] W. Hoogland *et. al.*, Nucl. Phys. **B126** (1977) 109.
- [28] C.D. Frogatt and J.L.Petersen, Nucl. Phys. **B129** (1977) 89.
- [29] J.F. Donoghue, E. Golowich and B.R. Holstein, *Dynamics of the Standard Model*, Cambridge University Press, 1992.

- [30] T. Appelquist and C. Bernard, Phys. Rev. **D 23** (1981) 425.
- [31] J. M. Namyslowski, Phys. Rev. **160** (1967) 1522.
- [32] S. Mandelstam, Phys. Rev. **112** (1958) 1344.
- [33] S. Weinberg, Phys. Rev. Lett **17** (1966) 616.
- [34] M. Knecht, B. Moussallam, J. Stern and N.H. Fuchs, Nucl. Phys. **B457** (1995)513; *ibidem* **B471** (1996)445;
- [35] J. Bijnens, G. Colangelo, G. Ecker, J. Gasser and M.E. Sainio, Phys. Lett. **B374** (1996) 210; *ibidem* Nucl. Phys. **B508** (1997) 263.
- [36] K. M. Watson, Phys. Rev. **95** (1955) 228.
- [37] L. Beldjoudi and T. N. Truong, hep-ph/9403348
- [38] Le viet Dung and T. N. Truong, hep-ph/9607378.
- [39] F. Guerrero and A. Pich, Phys. Lett. **B412** (1997) 382; F. Guerrero, Phys. Rev. **D57** (1998) 4136.
- [40] F. Guerrero and J. A. Oller, Nucl. Phys. **B537** (1999) 459.
- [41] R. Omnès, Nuovo Cimento **8** (1958) 316; N.I. Muskhelishvili, *Singular Integral Equations*, (1953) Noordhoff, Groningen.
- [42] J. Nieves and E. Ruiz Arriola, sent to Phys. Lett. **B**, hep-ph/9906437
- [43] G. Ecker et al., Phys. Lett. **B223** (1989) 425.
- [44] D. Morgan and M.R. Penninton, *The Second DAΦNE Physics Handbook* , Ed. L. Maiani, *et. al.*, (1995) 192.
- [45] S.R. Amendiola, *et. al.*, Nucl. Phys. **B277** (1986) 168 (NA7 collaboration).
- [46] L.M. Barkov, *et. al.*, Nucl. Phys. **B256** (1985) 365; and references therein.
- [47] J.L. Petersen, CERN Yellow Report **77-04** (1977).
- [48] M.J. Losty, *et. al.*, Nucl. Phys. **B69** (1974) 185.
- [49] O. Dumbrajs et al., Nucl. Phys. **B 216** (1983) 277.
- [50] J.A. Oller and E. Oset, Phys. Rev. **D60** (1999) 074023.
- [51] K. Kawarabayashi and M. Suzuki, Phys. Rev. Lett. **16** (1966) 255; Riazuddin and Fayyazuddin, Phys. Rev. **147** (1966) 1071.
- [52] T. N. Truong, Phys. Rev. Lett. **67** (1991) 2260.
- [53] R. Blakenbecler and R. Sugar, Phys. Rev. **142** (1966) 1051.
- [54] G.F. Chew and S. Mandelstam, Phys. Rev. **119** (1960) 467.
- [55] L. Castillejo, R. H. Dalitz and F. J. Dyson, Phys. Rev. **101** (1956) 453.
- [56] J. Stern, H. Sazdjian and N. H. Fuchs, Phys. Rev. **D 47** (1993) 3814.
- [57] J. Nieves and E. Ruiz Arriola, work in preparation.